Nanotoxicology

ISSN: (Print) (Online) Journal homepage: https://www.tandfonline.com/loi/inan20

Evaluation of the skin-sensitizing potential of gold nanoparticles and the impact of established dermal sensitivity on the pulmonary immune response to various forms of gold

K. A. Roach , S. E. Anderson , A. B. Stefaniak , H. L. Shane , G. R. Boyce & J. R. Roberts

To cite this article: K. A. Roach , S. E. Anderson , A. B. Stefaniak , H. L. Shane , G. R. Boyce & J. R. Roberts (2020) Evaluation of the skin-sensitizing potential of gold nanoparticles and the impact of established dermal sensitivity on the pulmonary immune response to various forms of gold, Nanotoxicology, 14:8, 1096-1117, DOI: 10.1080/17435390.2020.1808107

To link to this article: https://doi.org/10.1080/17435390.2020.1808107

NANOTOXICOLOGY
2020, VOL. 14, NO. 8, 1096–1117
https://doi.org/10.1080/17435390.2020.1808107

Taylor & Francis
Taylor & Francis Group

ORIGINAL ARTICLE

Evaluation of the skin-sensitizing potential of gold nanoparticles and the impact of established dermal sensitivity on the pulmonary immune response to various forms of gold

K. A. Roach[a], S. E. Anderson[a], A. B. Stefaniak[b], H. L. Shane[a], G. R. Boyce[a] and J. R. Roberts[a]

[a]Allergy and Clinical Immunology Branch (ACIB), National Institute of Occupational Safety and Health (NIOSH), Morgantown, WV, USA; [b]Respiratory Health Division (RHD), National Institute of Occupational Safety and Health (NIOSH), Morgantown, WV, USA

ABSTRACT

Gold nanoparticles (AuNP) are largely biocompatible; however, many studies have demonstrated their potential to modulate various immune cell functions. The potential allergenicity of AuNP remains unclear despite the recognition of gold as a common contact allergen. In these studies, AuNP (29 nm) dermal sensitization potential was assessed via Local Lymph Node Assay (LLNA). Soluble gold (III) chloride ($AuCl_3$) caused lymph node (LN) expansion (SI 10.9), whereas bulk particles (Au, 942 nm) and AuNP did not. Next, the pulmonary immune effects of AuNP (10, 30, 90 μg) were assessed 1, 4, and 8 days post-aspiration. All markers of lung injury and inflammation remained unaltered, but a dose-responsive increase in LN size was observed. Finally, mice were dermally-sensitized to $AuCl_3$ then aspirated once, twice, or three times with Au or AuNP in doses normalized for mass or surface area (SA) to assess the impact of existing contact sensitivity to gold on lung immune responses. Sensitized animals exhibited enhanced responsivity to the metal, wherein subsequent immune alterations were largely conserved with respect to dose SA. The greatest increase in bronchoalveolar lavage (BAL) lymphocyte number was observed in the high dose group – simultaneous to preferential expansion of BAL/LN CD8+ T-cells. Comparatively, the lower SA-based doses of Au/AuNP caused more modest elevations in BAL lymphocyte influx (predominantly CD4+ phenotype), exposure-dependent increases in serum IgE, and selective expansion/activation of LN CD4+ T-cells and B-cells. Overall, these findings suggest that AuNP are unlikely to cause sensitization; however, established contact sensitivity to gold may increase immune responsivity following pulmonary AuNP exposure.

ARTICLE HISTORY
Received 6 April 2020
Revised 1 June 2020
Accepted 9 June 2020

KEYWORDS
Nanotoxicology; allergic contact dermatitis; gold nanoparticles; pulmonary immune response; allergic sensitization

Introduction

Gold nanoparticles (AuNP) exhibit unique physical and chemical properties that render them exceptionally useful in many industrial applications. Similar to other metal nanomaterials, AuNP are becoming increasingly utilized as electrochemical sensors, antimicrobial coatings, catalysts, and fuel cell additives, with emerging applications in data storage and bioremediation (Yanez-Sedeno and Pingarron 2005; Zhang et al. 2015); however, the greatest demand for AuNP uniquely originates from the biomedical sector. As one of the few nanomaterials being extensively used in novel medical applications, 80% of all globally-manufactured AuNP is destined for use in healthcare-related end markets (Kumar and Roy 2016). AuNP exhibit general biocompatibility, are easily synthesized, and their physicochemical properties can be readily manipulated – all of which are characteristics underlying their proposed utility as a novel vaccine platform, diagnostic imaging agent, drug delivery vehicle, and adjuvant in cancer therapy, among other uses (Dreaden et al. 2012; Guo et al. 2017; Yamada, Foote, and Prow 2015; Zhang et al. 2009).

In accordance with current and emerging applications, the surge in global demand for gold nanomaterials is inevitably linked to increases in the risk of exposure. As greater numbers of workers become involved in the production, handling, transport, and disposal of AuNP, consumers and the

CONTACT K. A. Roach wvq1@cdc.gov Allergy and Clinical Immunology Branch (ACIB), National Institute of Occupational Safety and Health (NIOSH), 1095 Willowdale Drive, Morgantown, WV 26505, USA

Supplemental data for this article can be accessed here.

general public are more likely to come into contact with the materials being utilized in various end-market settings. Inhalation and dermal contact constitute the exposure routes of greatest concern for AuNP, and likewise, have been frequently investigated in nanotoxicological evaluations of the material (Thakor et al. 2011). Consequently, while AuNP have not been commonly implicated in overt toxic responses of the skin or airways, they have been shown to modulate various immune processes *in vitro* and *in vivo* (Bancos, Stevens, and Tyner 2015; Barreto et al. 2015; Chia-Hui et al. 2014; Hussain et al. 2011). These observations are concerning since some formulations of gold are known to cause diverse immunotoxic responses, one of which is an allergic disease (Aaron, Davis, and Percy 1985; Highton et al. 1981; Hunter 1985). Gold-induced allergic contact dermatitis (ACD) is the most common form of allergy to the metal in the general population (Davis et al. 2011; Fowler Jr. et al. 2001). Gold has also been occasionally implicated in systemic sensitization of patients undergoing gold therapy for the treatment of rheumatoid arthritis (Evans et al. 1987). Subsequent presentations of metal sensitivity are often limited to dermal eruptions elicited by subsequent treatments; however, a delayed-type hypersensitivity response of the airways termed 'gold lung' is also occasionally reported to emerge in these subjects (Evans et al. 1987).

Despite the established immunotoxic potential of gold salts, it remains unclear if AuNP may cause similar effects, such as the development of gold allergy. It also remains unknown whether AuNP exposure may induce allergic responses in subjects with existing sensitivity to gold. Moreover, since nanoscale materials exhibit an increased propensity for aerosolization, AuNP use constitutes the emergence of an unprecedented route of exposure to gold with unknown toxicological consequences (Evans et al. 2013). To begin addressing these knowledge gaps, three *in vivo* studies were conducted using a mouse model. First, the potential for AuNP to induce dermal sensitization was investigated using the Local Lymph Node Assay (LLNA) and compared to the immunogenic activity of soluble gold salts and larger particulate forms of gold. Next, the pulmonary immune effects of AuNP were assessed *in vivo* with respect to dose and time. Lastly, the impact of established dermal sensitivity on the pulmonary immune response to gold was investigated. Mice were aspirated with bulk gold particles or AuNP in mass- or surface area-normalized doses to determine if these parameters were related to subsequent biological effects. Collectively, the findings from these studies will help determine if AuNP exposure may lead to the development of the gold-specific allergic disease. Furthermore, the results will clarify whether individuals with existing dermal sensitivity to gold constitute a population increasingly vulnerable to adverse immune effects following respiratory AuNP exposure.

Materials and methods

Material characterization

Gold particles (<10 μm, Au) and gold (III) chloride ($AuCl_3$) were obtained from Sigma-Aldrich in powder form. Gold nanoparticles (AuNP) were obtained from the National Institute of Standards and Technology (NIST) Standard Reference Materials Program. Reference Material 8012 is a well-characterized citrate-stabilized AuNP (30 nm nominal diameter) received at a concentration of 20% (w/v) in aqueous suspension (NIST 2015). Physico-chemical properties of both particulate gold materials were characterized prior to incorporation into *in vivo* studies.

Primary particle size, agglomerate size, and particle morphology

Field emission scanning electron microscopy (FE-SEM, Hitachi Model S-4800) and transmission electron microscopy (Philips Electron Optics model CM30) were employed to assess the primary particle size and morphology of Au and AuNP. Particles were prepared in distilled water for microscopic analysis. Images were collected for both particles and using the SEM images, the diameters of 250 particles from each sample were recorded using point count methods. Image J Software (Version X; National Institutes of Health; Bethesda, MD) was used for the analysis of mean diameter for each particle.

Surface area

The surface area of the Au particles (in powder form) was measured by gas adsorption using a

Quantachrome NOVA 2200e surface area analyzer and ultra-high purity nitrogen adsorbate. Specific surface area (SSA) was determined by using the multipoint Brunauer, Emmett, and Teller (BET) method (American Society for Testing and Materials International 2002). Since AuNP were received in aqueous suspension, geometric calculations were used to determine the surface area of this material using the particle sizes generated from microscopic measurements and the known density of gold (19.32 g/cm^3). The same approach was employed with Au to confirm the results from gas adsorption analysis.

Endotoxin contamination

Endotoxin presence in the Au and AuNP samples was evaluated using the Pierce Limulus Amebocyte Lysate (LAL) Chromogenic Endotoxin Quantitation Kit (Thermo Scientific; Waltham, MA) according to the manufacturer's protocol. Both Au samples were tested over multiple concentrations ranging from 5.0–0.25 μg/μL. The concentration of endotoxin was then determined using a plate spectrophotometer at an absorbance wavelength of 450 nm.

Zeta potential in vehicle

Zeta potential of Au and AuNP particles was determined by measuring electrophoretic mobility in distilled water (pH 7.1). All measurements were performed at 25 °C using a Malvern Zetasizer Nano ZS90 (Worcestershire, UK) equipped with a 633 nm laser at a 90° scattering angle. Samples were equilibrated inside the instrument for 2 min, and five measurements consisting of five runs each were recorded.

Animals

Specific pathogen-free female C57BL/6J mice, 8–12 weeks of age, were obtained from Jackson Laboratory (Bar Harbor, ME) for use in all studies. All mice were housed 4 per cage in polycarbonate ventilated cages with HEPA-filtered air in the AAALAC International-approved National Institute for Occupational Safety and Health (NIOSH) Animal Facility and provided food (Harlan Teklad Rodent Diet 7913) and water ad libitum in a controlled humidity/temperature environment with a 12 h light/dark cycle. Animals were allowed to acclimate for four weeks in the facility prior to exposures. All procedures in the studies comply with the ethical standards set forth by the Animal Welfare Act and the Office of Laboratory Animal Welfare (OLAW). The studies were approved by the CDC-Morgantown Institutional Animal Care and Use Committee in accordance with approved animal protocols (13-SA-M-022, 18-001).

In vivo *exposures and study design*

Local lymph node assay

The Local Lymph Node Assay (LLNA) was performed in accordance with previously-established standardized protocols (Basketter et al. 2002). Accordingly, mice ($n = 8$ per group) were exposed topically to vehicle control (50% DMSO in distilled, deionized water), increasing concentrations of Au or AuNP, or positive control (10% $AuCl_3$) on the dorsal sides of both ears (25 μL per ear) for three consecutive days (days 1, 2, and 3) (Figure 1). Following two days of rest, on day 6, mice were injected intravenously via the lateral tail vein with 20 μCi [^{3}H]-thymidine (Dupont NEN, specific activity 2 Ci/mmol). Five hours after the [^{3}H]-thymidine injection, mice were euthanized via CO_2 asphyxiation and the left and right auricular lymph nodes (ALN) were excised from each mouse and pooled. Single-cell suspensions were prepared, and following overnight incubation in 5% trichloroacetic acid (TCA), samples were analyzed using a Packard Tri-Carb 2500TR liquid scintillation counter. Stimulation indices (SI) were calculated by dividing the mean disintegrations per minute (DPM) per test group by the mean DPM for the vehicle control group.

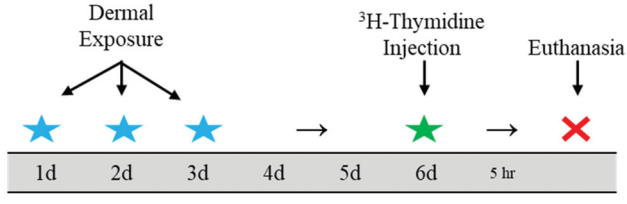

Figure 1. Timeline of exposures for the Local Lymph Node Assay (LLNA). Mice were dermally exposed to vehicle control (50% DMSO), positive control (10% $AuCl_3$), or 2.5, 5.0, or 10% Au or AuNP for three consecutive days on the dorsal sides of both ears. Following 2 days of rest, mice were injected intravenously with ^{3}H-thymidine, euthanized 5 h later, and the auricular lymph nodes were harvested for analysis.

AuNP dose-response study

AuNP were incorporated into a dose-response time course study in order to evaluate pulmonary toxicity and determine optimal doses for incorporation into the allergy study. AuNP were diluted in distilled water at concentrations of 0.2, 0.6, and 1.8 mg/mL and sonicated for 10 seconds at 10 W with a probe sonicator. On day 0, mice ($n = 8$ per group per time point) were exposed by the oropharyngeal aspiration to 50 μL of either solution to constitute three AuNP doses: 10, 30, or 90 μg. Mice were fully anesthetized with isoflurane, placed on a slanted board, and suspended by the incisors. The mouth was opened and tongue moved aside, while a 50 μL aliquot of sample was pipetted on the base of the tongue. The animal was restrained until two full breaths were completed and returned to its cage, placed on its side, and monitored for recovery from anesthesia. Mice were humanely euthanized with an overdose of sodium pentobarbital euthanasia solution (100–300 mg/kg body weight; Fort Dodge Animal Health; Fort Dodge, IA) at 1, 4, or 8 days post-exposure. Blood was collected from the abdominal aorta, bronchoalveolar lavage (BAL) was performed, and mediastinal lymph nodes (MLN) and spleens were collected for analysis.

Gold allergy model

In order to determine the effects of preexisting dermal sensitivity to gold on the pulmonary response to different forms of gold materials, an allergy study was conducted in two blocks. Treatment groups and schedule of exposures are shown in Figure 2.

(A)

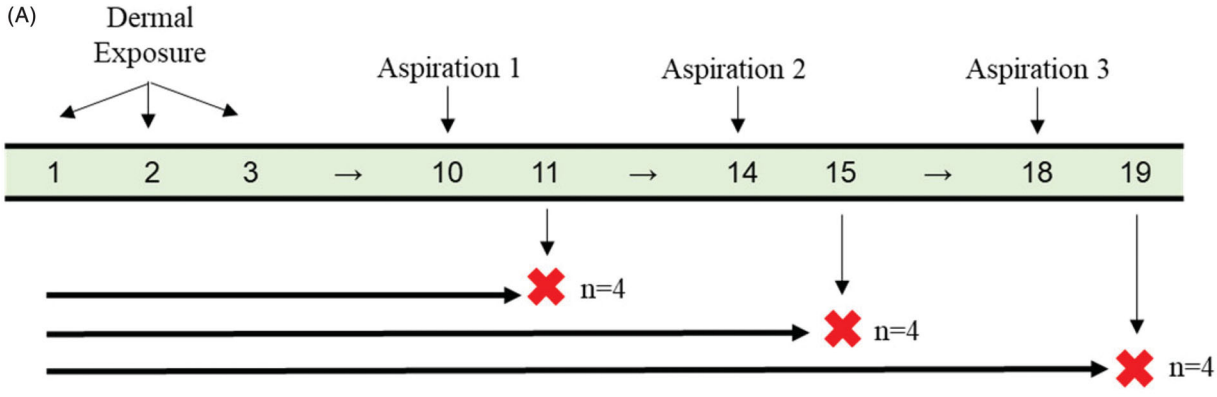

(B)

Gold Allergy Model
Treatment Groups and Corresponding Exposure Metrics

Treatment Group	Group #	Exposures			
		Days 1-3 (dermal)	Days 10, 14, 18 (aspiration)		
			Particle	Dose Mass	Dose SA
Non-sensitized, vehicle control	1	DMSO	VC	-	-
Non-sensitized, Au	2		Au (942 nm)	30 μg	8.40×10^{-6} m^2
Non-sensitized, mass-normalized AuNP	3		AuNP (30 nm)	30 μg	3.14×10^{-4} m^2
Non-sensitized, SA-normalized AuNP	4		AuNP (30 nm)	0.8 μg	8.40×10^{-6} m^2
Sensitized, vehicle control	5	10% $AuCl_3$	VC	-	-
Sensitized, Au	6		Au (942 nm)	30 μg	8.40×10^{-6} m^2
Sensitized, mass-normalized AuNP	7		AuNP (30 nm)	30 μg	3.14×10^{-4} m^2
Sensitized, SA-normalized AuNP	8		AuNP (30 nm)	0.8 μg	8.40×10^{-6} m^2

Figure 2. Schedule of exposures for the gold allergy study (A) and treatment groups with corresponding exposures (B). Mice were treated dermally with DMSO vehicle control (VC) or 10% $AuCl_3$ on days 1, 2, and 3 to establish contact allergy to gold in one set of animals (groups 5–8) and generate a set of nonsensitized control animals (groups 1–4). After 6 days of rest, mice were aspirated with H2O (VC), Au particles, or AuNP in mass- or surface area (SA)-normalized doses beginning on day 10. After the first aspiration (day 10), a set of mice from each group ($n = 4$) was euthanized the following day (day 11). The remaining mice were aspirated again with identical treatment doses on day 14, and a set of mice ($n = 4$) was euthanized the following day (day 15). The last group of mice were aspirated a third time on day 18 and euthanized the following day (day 19).

Mice (96 total) were randomly assigned to one of eight treatment groups. Beginning on day 1, using identical methods as those previously described for the LLNA, four groups of mice (groups 1–4) were dermally exposed to 50% DMSO and four groups were exposed to 10% $AuCl_3$ (groups 5–8). Exposures were repeated on days 2 and 3 to complete the sensitization procedure, and mice were then rested for 6 days. On day 10, control (non-sensitized) and gold-sensitized groups were paired and assigned one of four treatments. Exposure solutions were distilled water (vehicle control [VC], groups 1 and 5), 30 μg Au (groups 2 and 6), or AuNP at doses normalized for mass (30 μg, groups 3 and 7) or surface area (9.90×10^{-6} m^2, groups 4 and 8) of the Au exposure. After mice were aspirated with the corresponding dosing solutions once (day 10), twice (day 14), or three times (day 18), a set of mice from each group was euthanized the following day (days 11, 15, and 19; $n = 2$ per group per block $\times$ 2 blocks). Following sacrifice, serum was collected, BAL was performed, and immune tissues were collected for analysis ($n = 4$ animals per group per time point).

Toxicology and immune response parameters

BAL cellular and fluid analysis

BAL was performed on the lungs of mice from both the AuNP dose-response study and gold allergy study in order to obtain pulmonary cells for phenotypic analysis and fluid for analysis of biochemical indicators of lung injury and inflammation. Following euthanasia, the trachea was cannulated, the chest cavity was opened, and BAL was performed on the whole lungs. The acellular fraction of the first lavage was obtained by filling the lung with 0.6 mL PBS, massaging for 30 seconds, and withdrawing. This concentrated aliquot was retained, kept separate, and designated as the first fraction. The following aliquots were 0.6 mL in volume, instilled once with light massaging, withdrawn, and combined until a 2.4 mL volume was obtained. For each animal, both lavage fractions were centrifuged (10 min, 300 $\times$ *g*) and the cell pellets were combined and resuspended in 1 mL PBS for cell counts, phenotyping, and microscopic analysis. The acellular fluid from the first fraction (BALF) was retained for analysis of LDH activity and quantification of cytokines.

Total BAL cell number was determined using a Coulter Multisizer II (Coulter Electronics; Hialeah, FL) by quantifying the number of events within a size range of 4.5 μm and 20 μm. BAL cell subsets were visualized by spinning down 75 000 cells from each sample onto microscope slides using a Cytospin 3 centrifuge (Shandon Life Sciences International; Cheshire, England). Cells were labeled with Leukostat stain (Fisher Scientific; Pittsburgh, PA), and microscopic analysis allowed for differentiation between alveolar macrophages, eosinophils, lymphocytes, and neutrophils. An aliquot of BAL cells was also stained for surface markers to allow for phenotypic differentiation of lymphoid and myeloid immune cell populations by flow cytometry, using procedures described below.

Measurements of LDH activity in BALF were obtained using a Cobas Mira analyzer (Roche Diagnostic Systems; Montclair, IN) as an index of lung injury. LDH activity was quantified by detection of the oxidation of lactate coupled to the reduction of NAD + at 340 nm.

Lymphocyte differentials by flow cytometry

For the AuNP dose-response study and gold allergy study, lymph nodes and spleens were harvested from mice for characterization of immune cell populations within these tissues. In the AuNP dose-response study, only the MLN, which drain the lungs, were collected. In the gold allergy study, both the MLN and ALN were collected in order to compare cellular profiles in the local lymphoid tissues corresponding to the different sites of gold exposure. Spleens and lymph nodes were processed between frosted microscope slides to yield single-cell suspensions in sterile PBS. Concentrations of cells from each tissue were determined by identical methods used for the enumeration of BAL cells.

For flow cytometric analysis, 500 000 cells from each tissue were suspended in staining buffer (PBS + 1% bovine serum albumin + 0.1% sodium azide) containing F_c receptor blocking anti-mouse CD16/32 (BD Biosciences, San Diego, CA). Cells were incubated for 5 min, washed, and resuspended in staining buffer containing fluorochrome-conjugated antibodies.

Lymphocyte phenotypes were determined for BAL, lymph nodes, and spleen cells using a staining panel containing CD2-BV605, CD3-APC, CD4-FITC, CD8-PE, CD44-APC-R700, CD45-PerCP, CD45R(B220)-

PE-Cy7, and CD86-BV421 (BD Biosciences). These markers allowed for discrimination between populations of CD4+ T-lymphocytes, CD8+ T-lymphocytes, B-lymphocytes, and NK cells, as well as determine the corresponding activation state of T-cells and B-cells.

Another aliquot of BAL cells was stained using the second panel of markers to allow for the differentiation of myeloid cell subsets. CD11b-PE-CF594, CD11c-APC-R700, CD24-BV605, CD45-PerCP, CD64-PE, CD86-PE-Cy7, MHC II-BV515, Ly6G-APC, Siglec-F-APC-Cy7 (BD Biosciences) were employed to differentiate between eosinophils, neutrophils, macrophages, and dendritic cells (Misharin et al. 2013).

Cells were incubated for 30 min with the respective staining cocktails, washed, and fixed in 100 μL Cytofix Buffer (BD Biosciences). Compensation controls were prepared using corresponding cell types stained with a single fluorophore. For each sample, 100,000 events were recorded on an LSR II flow cytometer (BD Biosciences). In all analyses, doublet exclusion was performed and cellular populations were gated on using FSC-A × SSC-A parameters, prior to subsequent analysis. All data analysis was performed using FlowJo 7.6.5. Software (TreeStar Inc., Ashland, OR).

Whole blood cellular differentials

In the AuNP dose-response and gold allergy studies, blood was drawn from the abdominal aorta directly following euthanasia. A 100 μL aliquot of whole blood was retained in order to quantify circulating immune cells, and the serum fraction was separated from the remaining blood volume for protein analysis. Using the aliquot of whole blood, erythrocyte and leukocyte number were determined for each sample, and leukocytes were differentiated (lymphocytes, monocytes, neutrophils, eosinophils, and basophils) using an IDEXX ProCyte Dx Hematology Analyzer (IDEXX Laboratories; Westbrook, ME).

BAL fluid and serum proteins

The BALF and serum cytokine profiles of animals from the AuNP dose-response study and gold allergy study were characterized using a Milliplex MAP Kit magnetic bead panel (EMD Millipore Corporation, Billerica, MA) and analyzed on a Luminex 200 system (Luminex Corporation, Austin, TX). For both studies, prototypical T-helper (Th)1/17 and Th2 cytokines were quantified. Specific analytes included interleukin (IL)-2, 4, 5, 6, 10, 12p40, 12p70, 13, 17, eotaxin, tumor necrosis alpha (TNF-α), interferon-gamma (IFN-γ), and granulocyte-macrophage colony-stimulating factor (GM-CSF).

In the gold allergy study, serum was also used to assess levels of circulating IgE. Serum was diluted 1:10 and total IgE was assessed by ELISA using the Mouse IgE ELISA kit (Innovative Research; Novi, MI) according to manufacturer instructions.

Statistical analysis

Statistical analyses were conducted with GraphPad Prism version 7 (San Diego, CA). Results from all studies are expressed as means ± standard error and considered statistically significant at $p < 0.05$. For all studies, all treatment groups were compared by one-way analysis of variance (ANOVA) followed by Tukey's *post hoc* test.

Results

Material characterization

TEM and SEM micrographs of both gold particles are shown in Figure 3. SEM micrographs were used to assess average particle size, which was determined to be 942.1 nm for Au and 29.7 nm for AuNP. The micrographs also revealed that the particulate constituents of Au and AuNP both exhibited similar spherical morphologies and smooth surface textures.

Gas adsorption was performed on the Au powder, and BET analysis gave an SSA of 0.33 ± 0.13 m^2/g. Using the particle sizes determined from microscopy, geometric calculations indicated an SSA of 10.46 m^2/g for AuNP. Consistent with the results from gas adsorption/BET analysis, an SSA of 0.28 m^2/g was calculated for Au using the same approach. No detectable levels of endotoxin were present in either sample. Zeta potential was determined to be −26.4 ± 5.1 mV for Au and −33.6 ± 6.9 mV for AuNP. Results from the physicochemical characterization of Au and AuNP are summarized in Table 1.

LLNA study

Using 10% $AuCl_3$ as a positive control, the capacity for Au and AuNP to induce dermal sensitization was

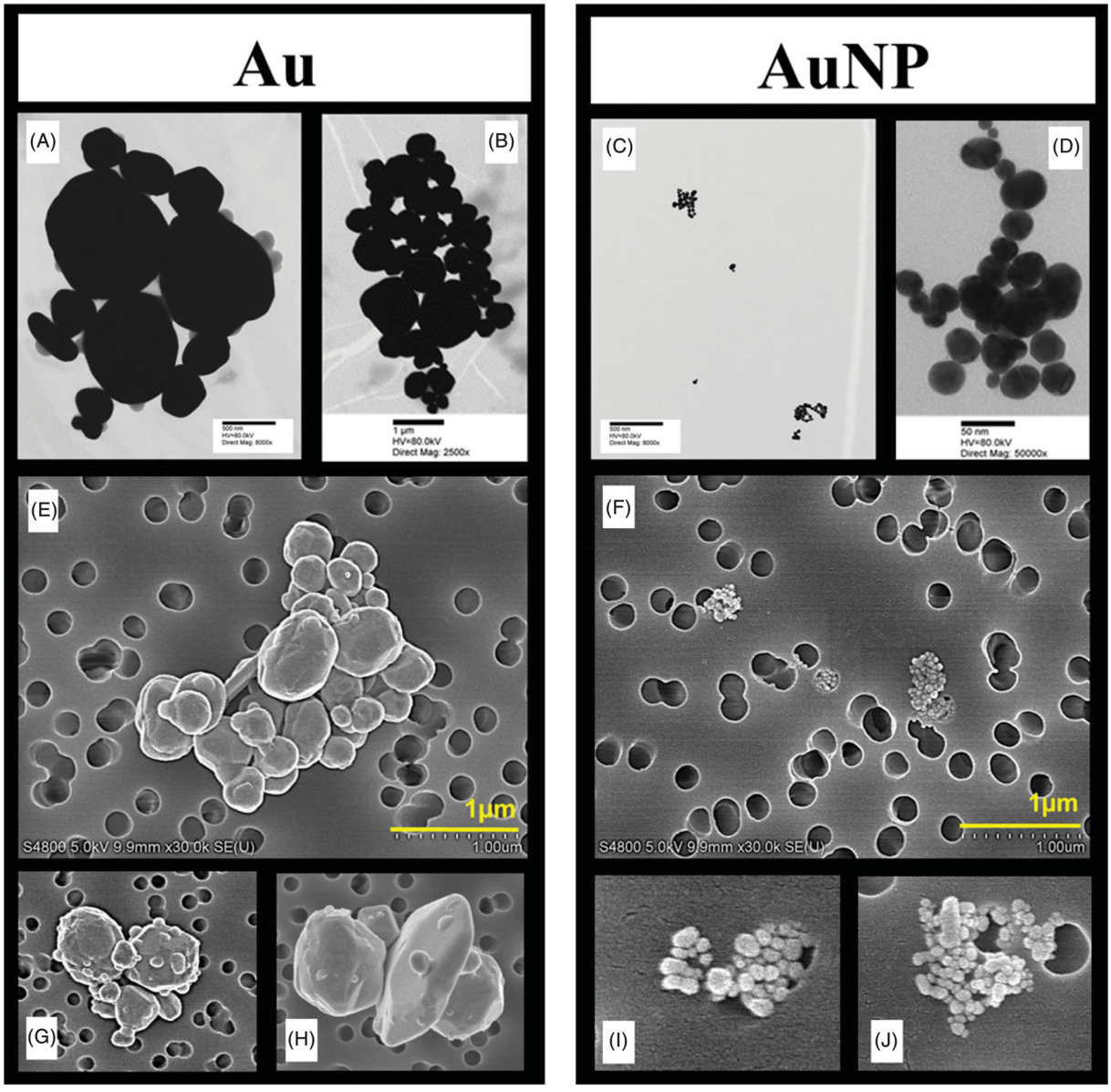

Figure 3. Transmission electron micrographs of Au (A, B) and AuNP (C, D). Particles are shown at equal magnifications in A and C (scale bar = 500 nm) and in size-specific detail in (B) (scale bar = 1µm) and (D) (scale bar = 50 nm). Scanning electron micrographs of Au (E, G, H) and AuNP (F, I, J) are shown below transmission micrographs. Particles are shown at equal magnifications in E and F (scale bar = 1µm) and size-adjusted magnifications to show particle surface detail in (G), (H), (I), and (J).

assessed using a standard procedure for the LLNA (Dearman, Basketter, and Kimber 1999). Mice were topically exposed to Au or AuNP in concentrations of 2.5, 5.0, or 10.0%, and subsequent lymphocyte proliferation was determined by measuring ^{3}H-thymidine levels in the ALN (Figure 4). $AuCl_3$ had a stimulation index (SI) of 10.9, consistent with previous investigations demonstrating significant lymphocyte expansion following *in vivo* exposure to the compound (Basketter et al. 1999; Ikarashi, Kaniwa, and Tsuchiya 2002). Although the SI of AuNP (2.3) was higher than that of Au (1.1), a three-fold increase in lymphocyte proliferation was not observed for either particle, indicating a lack of sensitizing potential.

AuNP dose-response study

The effect of AuNP exposure on the lungs was investigated in a dose-response time-course study. Mice were aspirated with VC or AuNP in 10, 30, or 90 µg doses and euthanized on days 1, 4, or 8 post-aspiration to evaluate markers of pulmonary injury and inflammation. Overall, AuNP caused minimal

Table 1. Summary of Au and AuNP Characterization Results.

	Au	AuNP
Vendor size specification	<10 μm	30 nm
Material form	Powder	Citrate-stabilized in H_2O (20% w/v)
Primary particle size	942.1 ± 42.1 nm	29.7 ± 1.2 nm
Morphology	Spherical	Spherical
SSA: gas adsorption/BET (powder)	0.33 ± 0.13 m^2/g	
SSA: geometric calculation	0.28 m^2/g	10.46 m^2/g
Endotoxin level	Not detected	Not detected
Zeta potential (mV)	−26.4 ± 5.1	−33.6 ± 6.9

Summary of results from physico-chemical characterization of gold particles (Au) and gold nanoparticles (AuNP).

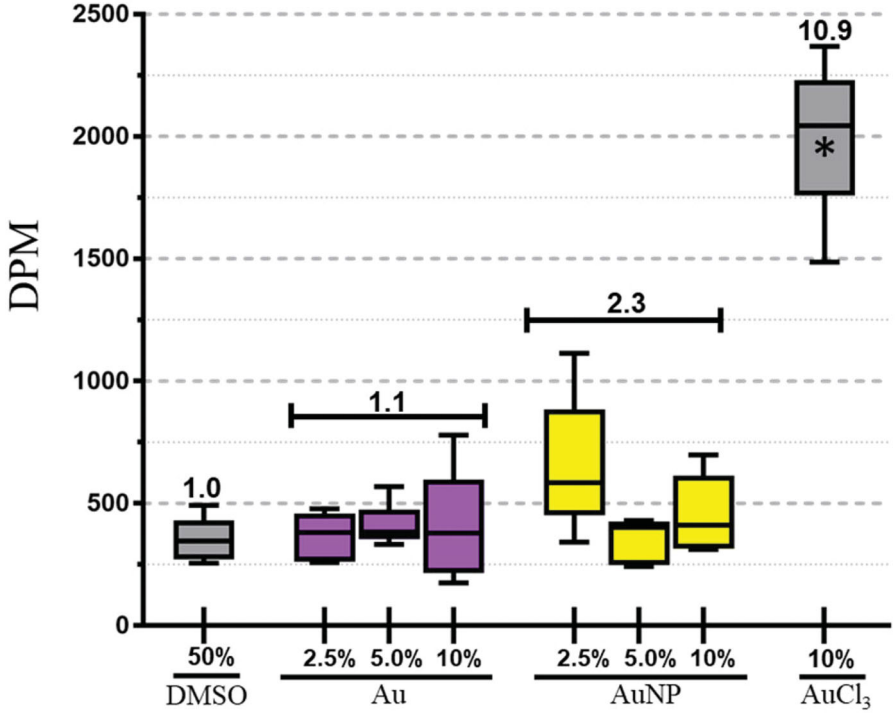

Figure 4. Results from the Local Lymph Node Assay (LLNA). The auricular lymph nodes were excised and ^{3}H-thymidine incorporation was assessed (expressed as disintegrations per minute [DPM]). Treatment groups included vehicle control (gray, 50% DMSO); Au (purple) or AuNP (yellow) in concentrations of 2.5, 5.0, or 10% (purple); and positive control (gray, 10% $AuCl_3$). Stimulation index was calculated for each material and is shown over the corresponding bars. $n = 8$ per group, $p < 0.05$, *indicates statistically significant from all other groups.

lung injury and inflammation. No increases in BALF LDH level were observed at any time point, irrespective of dose (Table 2). Similarly, total BAL cell number and BAL neutrophil number were not significantly increased in any groups on days 1, 4, or 8 post-aspiration.

A significant increase in MLN total cell number was observed at days 4 and 8 in animals exposed to the 90 μg dose of AuNP (Figure 5). Phenotypic analysis of these cells revealed that the increase in MLN cellularity involved the expansion of selective lymphocyte subsets (Table 3). Exposure to the highest dose of AuNP led to a significant increase in the proportion of CD4+ T-cells (65.8% compared to 61.9, 62.5, and 61.8%) and B-cells (16.1% compared to 12.9, 11.8, and 11.6%) at day 8 compared to all other groups. Simultaneously, a decrease in the proportion of CD8+ T-cells (16.7% compared to 23.2, 22.5, and 22.6%) was observed.

Despite alterations in lymphocyte population frequency in the MLN of animals exposed to the 90 μg AuNP dose, no alterations in the proportionality of CD4+ T-cells, CD8+ T-cells, B-cells, or NK cells were seen in the spleens of any groups at any time point (data not shown). Similarly, no significant alterations in the absolute number or proportion of circulating neutrophils, monocytes, eosinophils, basophils, or lymphocytes were observed between any groups at

Table 2. AuNP dose-response study markers of pulmonary inflammation.

Time point (days)	Treatment group	LDH (U/L)	Total # BAL, cells	Total # BAL, neutrophils
1	VC	73.1 ± 4.9	1 153 929 ± 162 306	7709 ± 978 (0.7%)
	10 μg AuNP	82.9 ± 6.8	1 094 438 ± 142 333	7334 ± 827 (0.7%)
	30 μg AuNP	76.5 ± 6.3	1 057 350 ± 143 786	6262 ± 759 (0.6%)
	90 μg AuNP	75.0 ± 4.4	1 103 788 ± 91 314	6058 ± 661 (0.6%)
4	VC	76.4 ± 4.4	1 097 086 ± 165 567	5199 ± 305 (0.5%)
	10 μg AuNP	67.8 ± 5.4	1 147 800 ± 161 494	7095 ± 935 (0.7%)
	30 μg AuNP	78.5 ± 6.9	1 142 613 ± 153 542	6229 ± 572 (0.6%)
	90 μg AuNP	72.0 ± 4.1	1 168 300 ± 176 462	6673 ± 693 (0.6%)
8	VC	79.3 ± 2.8	1 131 214 ± 170 708	6650 ± 586 (0.6%)
	10 μg AuNP	76.3 ± 3.0	1 080 338 ± 145 117	6782 ± 859 (0.6%)
	30 μg AuNP	80.8 ± 5.4	1 105 313 ± 161 021	7031 ± 651 (0.7%)
	90 μg AuNP	77.8 ± 4.2	1 256 250 ± 179 916	7016 ± 880 (0.6%)

Bronchoalveolar lavage (BAL) fluid lactate dehydrogenase (LDH) levels, total cell number, and total neutrophil number (and percent of total BAL cells) for each treatment group at 1, 4, and 8 days post-aspiration in the AuNP dose-response study. $n = 8$ per group.

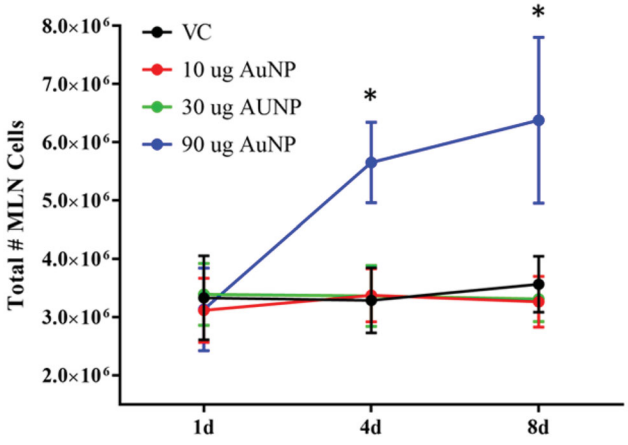

Figure 5. Mediastinal lymph node (MLN) cellularity with respect to time in the AuNP dose-response study. Total cell number is shown for each treatment group (black = vehicle control, red = 10 μg AuNP, green = 30 μg AuNP, blue = 90 μg AuNP) at each time point. $n = 8$ per group, $p < 0.05$, *indicates statistically significant from all other groups.

any time point. Moreover, BALF and serum cytokine concentrations were not altered in any group at any time point (data not shown).

Gold allergy model

Next, an allergy study was conducted in order to determine if existing dermal sensitivity to gold impacted the immune response following pulmonary exposure to Au and AuNP. In order to evaluate the role of particle size, dose mass, and surface area on any subsequent effects, mass, and surface area-normalized doses of Au and AuNP were used in the study. Treatment groups for the gold allergy study, corresponding Au/AuNP dose parameters, and a timeline of exposures are shown in Figure 2.

Quantification of BAL cells revealed no differences in total cell numbers between any non-sensitized groups (groups 1–4), irrespective of the number of gold aspirations. In gold-sensitized mice (groups 5–8), total BAL cell number did not differ between any groups after a single aspiration (day 11), but increased subsequently with each successive aspiration in a surface area-dependent manner (Figure 6(A)). By day 19, group 7 animals exhibited the greatest number of total BAL cells, which was statistically significant from all other groups.

Phenotypic differentiation of immune cell subsets within the BAL revealed similar increases in the number of neutrophils in all sensitized, gold-aspirated groups at day 15 (Figure 6(B), Table S1). Further increases in cell numbers were seen following the third aspiration in groups 6 and 7, ultimately resulting in 19th day BAL neutrophil values that were conserved between groups exposed to mass-normalized doses of gold. BAL eosinophil number was only elevated in group 7 at day 15, but by day 19, group 6 values also became significantly increased over group 5 (Figure 6(C)). The total number of lymphocytes recovered from the BAL of the sensitized groups increased with each successive aspiration of gold (Figure 7(A)). The extent of lymphocyte influx appeared dependent on the surface area of the administered dose of gold, and accordingly, the highest number of BAL lymphocytes was consistently seen in group 7.

BAL lymphocyte populations were further differentiated into B-cell and T-cell subtypes. Accordingly, the previously sensitized, gold-aspirated groups showed selective increases in phenotypically-distinct T-cell subsets within the BAL – an effect that appeared associated with dose surface area. The elevated number of BAL lymphocytes seen in groups 6 and 8 reflected a preferential increase in

Table 3. AuNP dose-response study mediastinal lymph node cell phenotypes by absolute number and percent of total cells.

Time point (days)	Treatment group	Total cell number	CD4+ T-cells	CD8+ T-cells	B-Cells	Other
1	VC	3 330 375 ± 256 150	2 069 951 ± 148 175 (62.3%)	744 929 ± 60 856 (22.5%)	408 346 ± 39 790 (12.5%)	107 148 ± 24 151 (3.1%)
	10 μg AuNP	3 117 500 ± 194 897	1 915 841 ± 124 602 (61.4%)	689 039 ± 45 979 (22.7%)	394 909 ± 21 226 (12.8%)	117 711 ± 20 734 (3.7%)
	30 μg AuNP	3 391 375 ± 187 436	2 094 021 ± 102 621 (61.9%)	759 018 ± 35 271 (22.5%)	435 524 ± 28 578 (12.2%)	102 812 ± 41 884 (2.7%)
	90 μg AuNP	3 133 875 ± 251 741	1 914 984 ± 146 250 (61.4%)	722 586 ± 74 333 (22.4%)	399 845 ± 37 158 (12.1%)	96 460 ± 18 594 (3.9%)
4	VC	3 286 000 ± 198 272	2 007 940 ± 127 193 (61.1%)	742 570 ± 45 135 (22.6%)	413 763 ± 16 308 (12.9%)	121 728 ± 29 422 (3.6%)
	10 μg AuNP	3 376 000 ± 161 796	2 081 110 ± 81 204 (61.8%)	786 458 ± 40 451 (23.3%)	418 648 ± 46 010 (12.3%)	89 784 ± 18 510 (2.8%)
	30 μg AuNP	3 364 875 ± 185 228	2 090 384 ± 101 344 (62.3%)	759 921 ± 26 892 (22.8%)	411 172 ± 32 564 (12.2%)	103 399 ± 38 202 (2.8%)
	90 μg AuNP	5 654 250 ± 243 934*	3 619 255 ± 185 728* (63.9%)	1 182 106 ± 92 905* (20.8%)	717 081 ± 40 146* (12.8%)	135 809 ± 58 070 (2.7%)
8	VC	3 564 875 ± 169 683	2 184 979 ± 103 467 (61.9%)	827 744 ± 46 725 (23.2%)	445 043 ± 23 599 (12.9%)	107 109 ± 25 372 (3.5%)
	10 μg AuNP	3 265 750 ± 154 216	2 036 649 ± 110 085 (62.5%)	731 991 ± 30 526 (22.5%)	387 887 ± 23 856 (11.8%)	109 224 ± 38 193 (3.4%)
	30 μg AuNP	3 312 000 ± 137 890	2 044 800 ± 78 954 (61.8%)	756 309 ± 43 031 (22.6%)	380 299 ± 15 133 (11.6%)	130 592 ± 36 204 (3.8%)
	90 μg AuNP	6 380 125 ± 503 521*	4 183 581 ± 339 718* (65.8%)	1 035 388 ± 83 588* (16.7%)	1 019 359 ± 82 338* (16.1%)	141 797 ± 37 995 (2.6%)

Phenotypic differentiation of lymphocyte subsets within the mediastinal lymph nodes (MLN) in the AuNP dose-response study. Absolute cell number for each lymphocyte subset is shown for all groups and time points. Subpopulation frequency is also shown next to the respective values. Lymphocyte subset proportionality is expressed as a percentage of total MLN cells for each group at each time point. $n = 8$ per group, $p < 0.05$.
*Indicates statistically significant from all other groups.

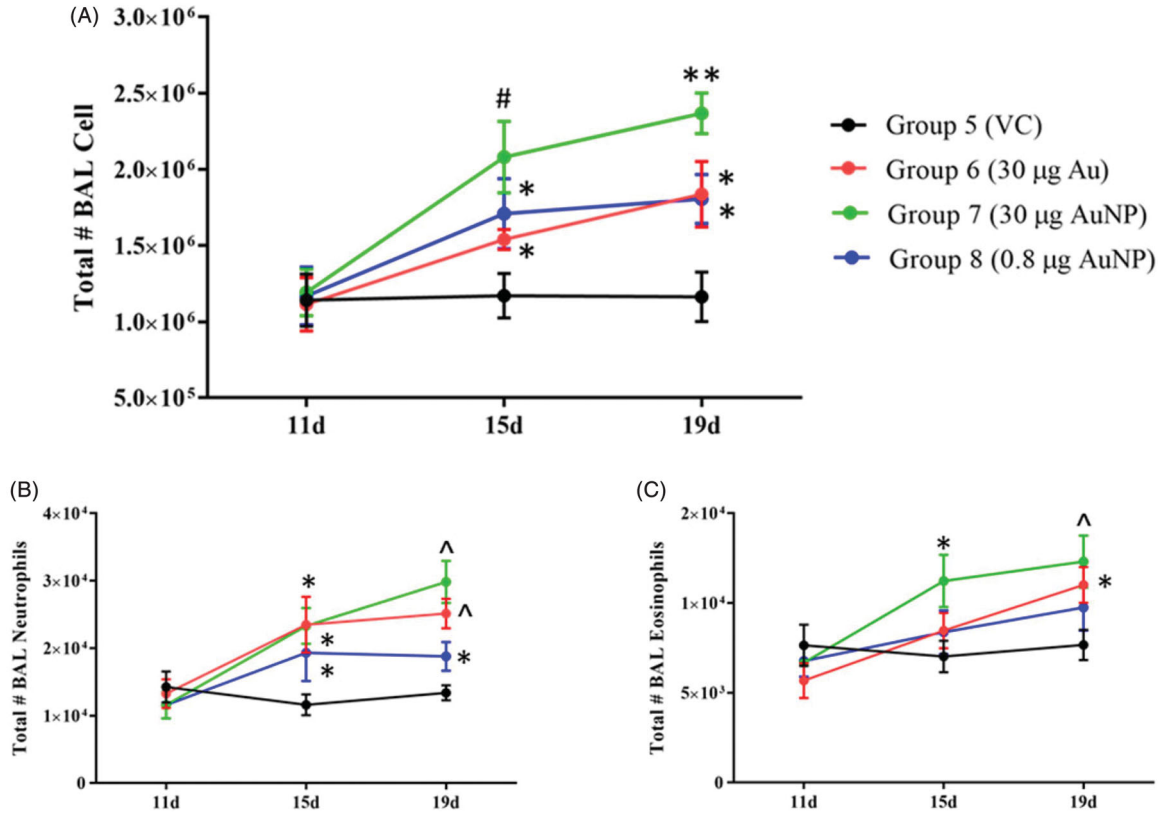

Figure 6. Total number of BAL cells in sensitized groups (groups 5–8) at all time points in the gold allergy model (A). Total number of BAL neutrophils (B) and eosinophils (C) are also shown for each time point. The total number of BAL cells, neutrophils, and eosinophils did not differ significantly between any nonsensitized groups (groups 1–4) or from group 5 control values at any time point. $n = 4$ per group, $p < 0.05$. *indicates statistically significant over group 5 control, **indicates statistically significant from all other groups, #indicates statistically significant from groups 5 and 6, ^ indicates statistically significant from groups 5 and 8.

CD4+ T-cells. Irrespective of increased cellular influx, the BAL CD4:CD8 T-cell ratio in groups 6 and 8 remained largely conserved with that of group 5 controls throughout the study (Figure 7(B,C)). By comparison, group 7 animals not only exhibited the greatest total number of BAL lymphocytes, but also an exclusive increase in the number and proportion of BAL CD8+ T-cells (2.10% of total BAL cells compared to 0.66, 0.75, and 0.81% in groups 5, 6, and 8, respectively) after three aspirations of gold. Correspondingly, a drastic decrease in the group's BAL CD4:CD8 T-cell ratio was evident at day 19.

Similar to the cellular responses observed in the lung, there were no alterations in MLN total cell number or ratios of lymphocyte populations in nonsensitized groups (groups 1–4) at any time point

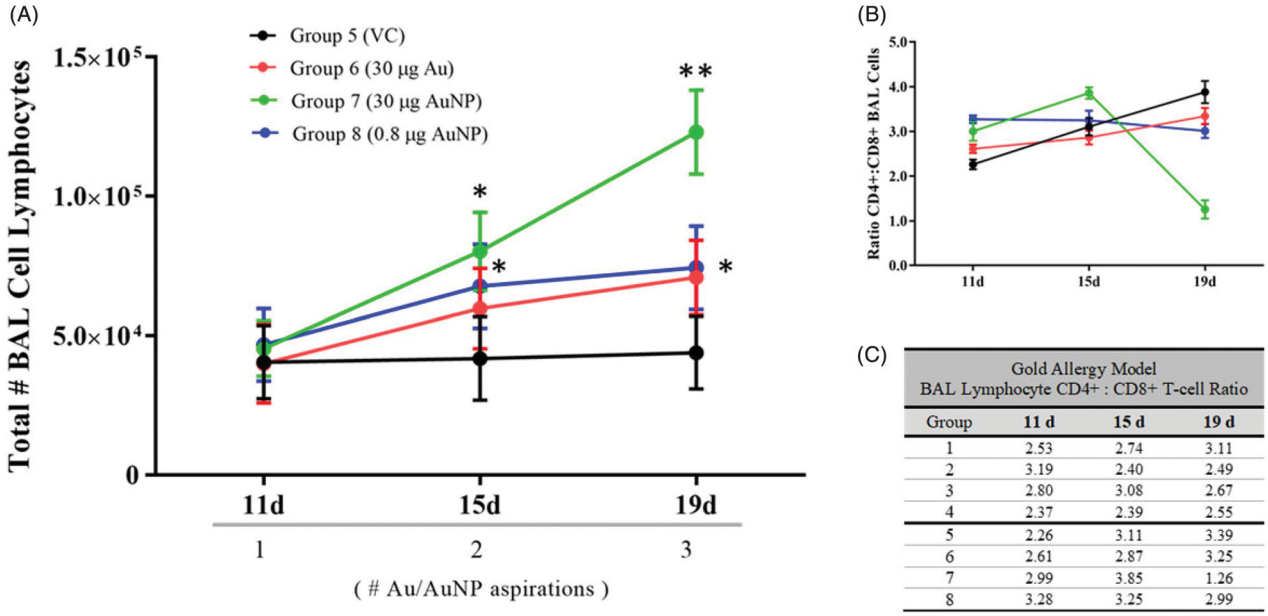

Gold Allergy Model
BAL Lymphocyte CD4+ : CD8+ T-cell Ratio

Group	11 d	15 d	19 d
1	2.53	2.74	3.11
2	3.19	2.40	2.49
3	2.80	3.08	2.67
4	2.37	2.39	2.55
5	2.26	3.11	3.39
6	2.61	2.87	3.25
7	2.99	3.85	1.26
8	3.28	3.25	2.99

Figure 7. Total number of BAL lymphocytes in sensitized groups of the gold allergy study (A). Exposuredependent alterations in BAL CD4: CD8 T-cell ratio are also shown for sensitized groups in (B) and for all groups in (C). $n = 4$ per group, $p < 0.05$. *Indicates statistically significant over group 5 control, **indicates statistically significant from all other groups at the corresponding time point.

Table 4. Gold allergy model mediastinal lymph node cell phenotypes by percent.

	Group							
	Non-sensitized				Sensitized			
Cell phenotype	1	2	3	4	5	6	7	8
Day 11								
Total LN Cell #	3 303 500	3 320 500	3 370 250	3 130 500	3 268 000	3 204 500	3 365 000	3 376 250
CD4+ T-cells	62.24%	63.35%	63.01%	61.49%	63.21%	62.22%	61.17%	62.59%
$CD44^{hi}$	1.23%	2.22%	1.49%	0.87%	1.17%	2.04%	2.39%	1.37%
CD8+ T-cells	22.4%	21.19%	20.58%	22.96%	22.19%	21.17%	23.69%	22.01%
$CD44^{hi}$	2.14%	1.47%	3.10%	2.85%	2.00%	3.15%	1.85%	1.96%
B-cells	12.55%	11.96%	13.22%	12.84%	12.22%	11.39%	22.01%	12.50%
$CD86^{hi}$	3.27%	4.18%	2.97%	3.11%	3.19%	2.87%	3.64%	2.45%
Other	2.22%	3.02%	2.35%	2.45%	2.38%	3.10%	1.69%	2.90%
Day 15								
Total LN Cell #	3 252 750	3 419 500	3 235 500	3 263 750	3 457 000	4 967 750*	5 683 500*	3 195 850
CD4+ T-cells	62.50%	62.59%	63.17%	61.97%	62.25%	63.12%	58.64%**	62.79%
$CD44^{hi}$	2.12%	2.14%	0.85%	1.49%	1.22%	3.36%	7.47% #	12.15%**
CD8+ T-cells	21.89%	22.59%	23.70%	22.60%	22.89%	22.96%	26.12%**	21.47%
$CD44^{hi}$	1.80%	1.66%	2.58%	3.10%	1.47%	2.59%	12.54%**	3.98%
B-cells	13.21%	12.45%	12.40%	11.88%	12.45%	11.24%	10.23%	11.95%
$CD86^{hi}$	3.00%	2.67%	2.41%	1.92%	2.22%	2.68%	2.77%	3.28%
Other	2.77%	3.08%	3.19%	2.71%	2.79%	2.68%	6.01%**	2.79%
Day 19								
Total LN Cell #	3 381 750	3 466 500	3 590 750	3 561 000	3 565 250	5 585 500*	6 443 000^	4 226 250
CD4+ T-cells	59.64%	61.27%	62.89%	62.99%	61.87%	62.39%	55.10%**	61.88%
$CD44^{hi}$	1.90%	0.85%	2.60%	2.31%	2.29%	26.9% @	14.23%*	24.47% @
CD8+ T-cells	21.90%	22.48%	23.57%	24.06%	22.89%	20.47%	31.12%**	23.41%
$CD44^{hi}$	1.88%	1.75%	1.67%	2.91%	2.05%	4.58%	35.21%**	5.12%
B-cells	12.56%	12.56%	13.14%	11.90%	12.45%	12.52%	9.56%	13.07%
$CD86^{hi}$	2.25%	2.49%	1.58%	0.88%	1.44%	25.51% @	5.55%*	20.19% @
Other	3.21%	1.86%	2.54%	2.31%	2.79%	3.21%	4.22%	1.64%

Mediastinal lymph node (MLN) lymphocyte phenotypes expressed as a percent of total cells for all groups at all time points in the gold allergy study. Activation status is also shown below each subset, and is expressed as a percentage of the total corresponding cell population expressing elevated levels of activation markers. $n = 4$ per group, $p < 0.05$.
*Indicates statistically significant from group 5 control, **indicates statistically significant from all other groups, #indicates statistically significant from groups 5 and 6, ^indicates statistically significant from groups 5 and 8, @indicates statistically significant from groups 5 and 7.

(Table 4). In sensitized groups, no alterations occurred after a single aspiration, but several features of the MLN cellular profile were altered after two and three aspirations of gold. On day 15, total MLN cell number was significantly increased in groups 6 and 7 compared to groups 5 and 8

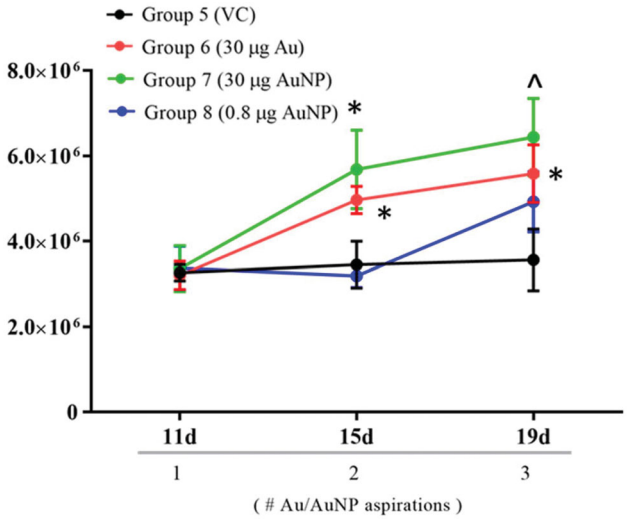

Figure 8. Mediastinal lymph node (MLN) size in sensitized groups of the gold allergy model at all time points. MLN size did not differ significantly between any non-sensitized groups (groups 1–4) or from group 5 control values at any time point. $n = 4$ per group, $p < 0.05$. *Indicates statistically significant from group 5 control, ^indicates statistically significant from groups 5 and 8.

(Figure 8); however, lymphocyte population ratios changed only in group 7 (Table 4). The nodes of these animals consisted of a lower proportion of CD4+ T-cells and a higher proportion of CD8+ T-cells and non-lymphoid cells when compared to all other groups at this time point. Group 7 animals also exhibited higher levels of CD4+ and CD8+ T-cells bearing a $CD44^{hi}$ phenotype. Interestingly, group 8 animals exhibited the highest proportion of $CD44^{hi}$ CD4+ T-cells among all groups.

After the third aspiration, MLN size remained elevated in groups 6 and 7, and while a slight increase in cellularity was observed in group 8 animals, the response was not statistically significant. At day 19, the MLN of all three sensitized/gold-aspirated groups contained greater numbers of activated CD4+ T-cells, CD8+ T-cells, and B-cells compared to group 5 controls. However, a higher proportion of activated CD4+ T-cells and B-cells was observed in groups 6 and 8, whereas the highest prevalence of activated CD8+ T-cells was seen in group 7. Numbers of activated CD4+ and CD8+ T-cells in the MLN of all sensitized groups are shown in Figure 9(A,B), respectively. The flow cytometry gating strategy used to discriminate CD44 expression levels and the degree of cellular activation is shown in Figure 9(C,D).

In addition to the MLN, the ALN was also collected from animals in the gold allergy model. Total ALN cell number was considerably elevated in all sensitized groups compared to all non-sensitized groups at every time point, consistent with previous exposure to $AuCl_3$. No significant alterations in ALN cellularity were observed in any group at any time point. Moreover, no significant differences in ALN size were observed amongst sensitization status-conserved groups. The ALN of naïve animals (groups 1–4) consisted of, on average, $\sim 3.5 \times 10^6$ total cells at days 11, 15, and 19. ALN collected from sensitized animals of groups 5–8 exhibited consistent cellularity throughout the time course as well, measuring $\sim 15.5 \times 10^6$ at all time points.

Phenotypic analysis of ALN lymphocyte populations also revealed sensitization state-dependent alterations in the proportionality of immune cell subsets in the local lymphoid tissue following dermal sensitization. Similar to ALN size, no alterations in lymphocyte subset proportionality were observed in any groups throughout the study, irrespective of gold aspiration frequency. Compared to non-sensitized groups, sensitized animals exhibited an elevated proportion of CD4+ (~67.5% of total ALN cells compared to ~61.0%) and CD8+ T-cells (~29.5% compared to 21.0%) and decreased ratio of B-cells (~8.8% compared to ~14.3%) (Table S2).

In the spleen, no alterations in lymphocyte population proportionality or activation status were observed between groups until day 15. At this time point, the only observable discrepancy was the frequency of activated CD4+ T-cells, which was elevated only in group 7 animals. By day 19, this group also exhibited an elevated proportion of CD8+ T-cells, higher levels of activated CD8+ T-cells, and a lower proportion of B-cells compared to all other sensitized groups. At the same time point, an increase in the number of B-cells expressing a $CD86^{hi}$ phenotype was observed in groups 6 and 8 (Table S3). Circulating immune cell populations were not altered in any group at any time point in the allergy study (data not shown).

Quantification of serum IgE revealed that previous sensitization procedures were associated with increased circulating antibody levels (Figure 10). After a single aspiration (day 11), all sensitized groups (groups 5–8) exhibited higher serum concentrations of total IgE than all non-sensitized

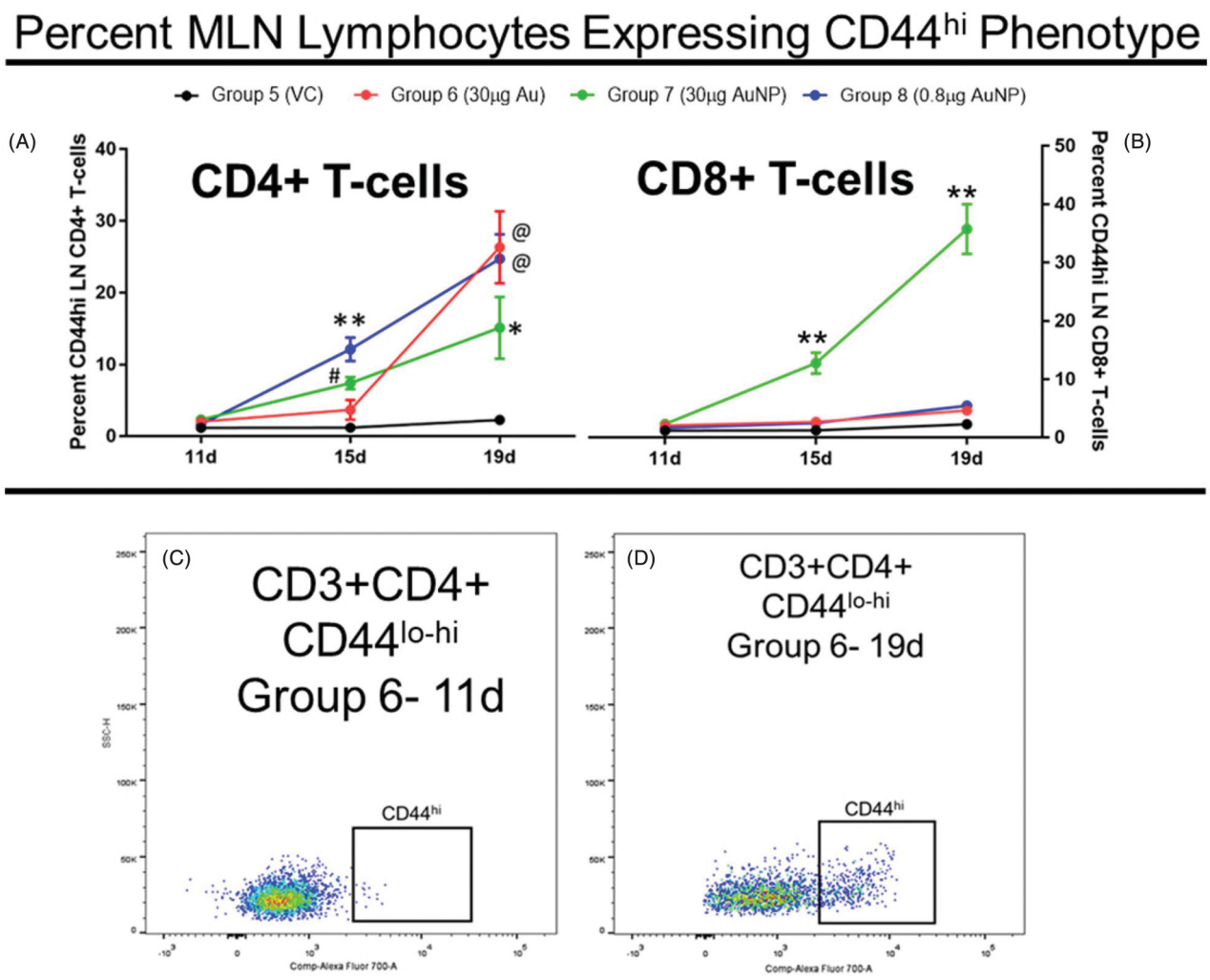

Figure 9. Mediastinal lymph node (MLN) lymphocyte activation status in the gold allergy study. Percent of MLN CD4+ T-cells (A) and CD8+ T-cells (B) expressing a CD44hi phenotype (indicative of cellular activation) at all time points for all sensitized groups. $n = 4$, $p < 0.05$. *Indicates statistically significant from group 5 control, **indicates statistically significant from all other groups, #indicates statistically significant from groups 5 and 6, @indicates statistically significant from groups 5 and 7. Flow cytometry gating strategy and population shift with respect to CD44 expression (group 6 CD3 + CD4+ cells at 11 days [C] and 19 days [D]) are shown.

groups (groups 1–4); however, no significant differences were observed between groups 5–8. Subsequent aspiration exposures did not impact IgE levels in groups 1–4, 5, or 7. By comparison, IgE levels increased in the serum of groups 6 and 8 with each successive aspiration, resulting in significant elevations over group 5 and 7 values by day15.

In non-sensitized groups of the allergy study, no alterations in serum cytokine levels were detected at any time point (Table 5). In previously-sensitized groups, the only significant change observable at day 15 was the concentration of IL-4 in the serum, which was significantly increased in group 6 animals over all other sensitized groups. A similar increase emerged in group 8 animals, but not until the 19th day time point. At the same time point, serum IL-10 levels were significantly elevated in groups 7 and 8, while increased IL-5 levels were exclusively seen in group 6.

Similar to their serum cytokine profiles, non-sensitized groups of the allergy study showed no changes in BALF cytokine concentrations at any time point (Table 6). Among dermally-sensitized groups, the only significant responses observed at day 15 included an increase in levels of GM-CSF and IL-6, seen in group 7 and group 6 animals, respectively. Following the third aspiration (day 19), BALF IL-12p70 and IL-2 levels became significantly increased in groups 7 and 8. BALF IFN-γ concentrations were elevated in all three sensitized, gold-

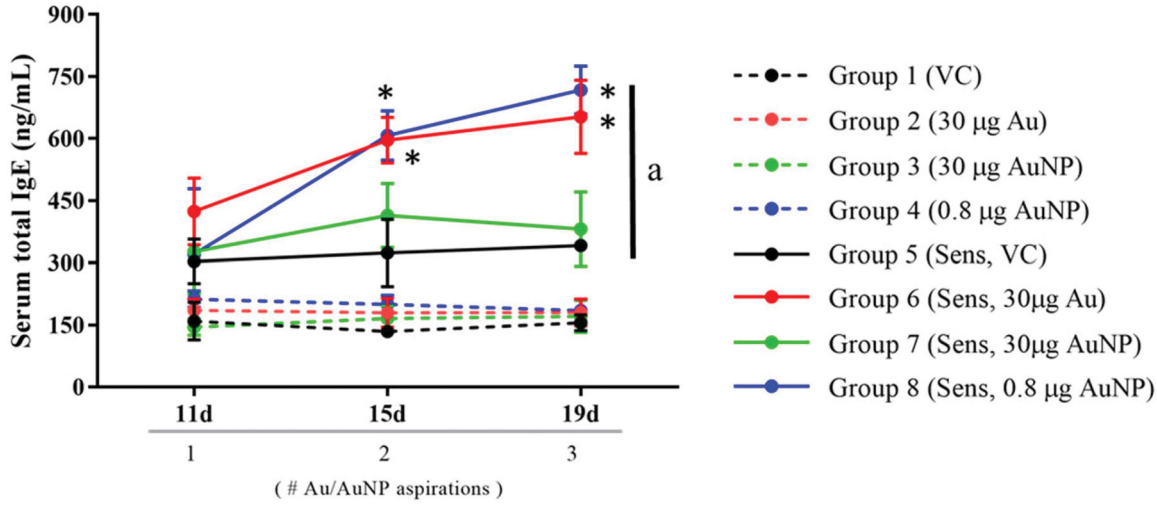

Figure 10. Circulating total IgE levels in all groups of the gold allergy study at all time points. Colormatched lines represent sensitized (solid line) and non-sensitized (dotted line) treatment-matched groups. $n = 4$ per group, $p < 0.05$. *Indicates statistically significant over group 5 control, 'a' indicates statistically significant from all non-sensitized control groups.

aspirated groups compared to group 5 control levels, but group 6 and 8 responses were further increased over that of group 7.

Discussion

In these studies, the immunogenicity of AuNP was examined *in vivo* to address different aspects of allergic disease. First, Au and AuNP were incorporated into an LLNA to evaluate their potential to induce skin sensitization. Neither particulate material was associated with significant lymph node expansion following dermal exposure at the selected doses (2.5–10%), indicating minimal risk for the development of gold-induced ACD. Next, a pulmonary dose-response study was performed to evaluate the inflammogenic potential of AuNP in the lungs. Even at the highest dose of 90 µg, no indications of pulmonary injury or inflammation were detected over the 8 day time course. The only observed alteration was a dose-responsive increase in MLN size at 4 and 8 days post-exposure. Finally, a third study was performed to evaluate the pulmonary response to gold particles in a state of established skin sensitivity. The results from this study demonstrated that dermal sensitization prior to respiratory exposure greatly impacted the immunological activity of gold in the lung. Furthermore, several local and peripheral immune markers were differentially impacted by various parameters of the administered dose of gold.

The outermost layers of the epidermis constitute a physical barrier that restricts many potential immunotoxicants from reaching the immunologically-active layers of the skin. In the context of skin allergy, this protective efficacy represents a major barrier responsible for limiting the sensitizing potential of many agents. The stratum corneum adequately restricts permeation of most high molecular weight and protein allergens, illustrating why the majority of contact sensitizers are reactive, low molecular weight chemicals and lipophilic molecules (Karlberg et al. 2008). Correspondingly, it has been suggested that nanomaterials may constitute a particular hazard for skin sensitization, given the size-dependent defensive functions of the epidermal barrier in ACD (Yoshioka et al. 2017). A general consensus regarding the skin-penetrating potential of nanomaterials has yet to be reached; however, a few studies have suggested that the size profile of nanomaterials results in enhanced dermal bioaccessibility, which can promote the development of skin allergy (Kim et al. 2013; Piasecka-Zelga et al. 2015). Contrary to these findings, the results from the LLNA study indicate that nanoscale dimensions do not confer increases in gold's sensitizing potential, as evidenced by similar degrees of lymphocyte expansion following exposure to Au and AuNP.

Although particle size did not appear to be a parameter critically-influential in the immunogenic activity of gold in the LLNA, the study results are consistent with the knowledge that many

Table 5. Gold allergy model serum cytokine levels (pg/mL).

Time point (days)	Tx group	Th1/Th17 cytokines							Th2 cytokines				Other	
		IFN-γ	IL-2	IL-12p40	IL-12p70	IL-17	TNF-α	GM-CSF	IL-4	IL-5	IL-13	Eotaxin	IL-6	IL-10
11	1	5.5 ± 1.1	12.0 ± 2.3	108 ± 11.2	49.8 ± 4.0	12.4 ± 2.2	36.1 ± 4.0	175 ± 22.3	3.0 ± 0.4	20.7 ± 2.2	411 ± 85.2	704 ± 95.3	36.5 ± 2.8	85.6 ± 9.6
	2	5.2 ± 1.3	10.4 ± 1.5	87.7 ± 10.1	55.7 ± 5.1	16.1 ± 1.9	29.4 ± 4.5	196 ± 31.8	2.5 ± 0.5	17.0 ± 1.9	364 ± 54.0	655 ± 120	30.2 ± 3.0	84.1 ± 8.8
	3	5.3 ± 1.2	11.8 ± 2.4	91.0 ± 10.1	61.0 ± 5.7	15.7 ± 3.0	37.0 ± 3.3	210 ± 29.9	2.4 ± 0.6	15.6 ± 2.0	385 ± 27.4	663 ± 94.2	31.1 ± 3.2	78.1 ± 7.1
	4	6.1 ± 2.0	10.0 ± 2.0	96.5 ± 15.6	46.5 ± 4.9	14.4 ± 1.8	33.4 ± 2.9	207 ± 18.7	1.9 ± 0.5	18.4 ± 1.6	399 ± 36.6	680 ± 76.0	29.9 ± 2.7	92.2 ± 7.7
	5	4.8 ± 1.6	14.7 ± 1.4	105 ± 15.5	45.5 ± 4.1	15.5 ± 1.7	30.5 ± 2.8	200 ± 24.5	2.2 ± 0.3	19.9 ± 1.7	421 ± 41.2	710 ± 110	42.1 ± 6.1	107 ± 11.4
	6	4.9 ± 1.2	12.2 ± 2.1	102 ± 17.5	55.7 ± 5.0	15.0 ± 1.9	41.1 ± 4.5	189 ± 20.3	2.3 ± 0.4	22.1 ± 1.5	404 ± 40.7	685 ± 103	40.0 ± 5.2	111 ± 10.5
	7	5.2 ± 1.0	13.3 ± 2.2	111 ± 20.1	52.9 ± 7.4	15.0 ± 1.8	32.2 ± 5.1	182 ± 15.6	3.1 ± 1.0	21.7 ± 3.4	371 ± 39.5	660 ± 99.7	38.8 ± 3.5	87.4 ± 6.2
	8	5.6 ± 0.9	10.9 ± 1.7	96.6 ± 14.4	56.6 ± 6.0	13.7 ± 2.3	37.0 ± 3.8	194 ± 19.1	2.6 ± 0.6	20.1 ± 2.1	385 ± 28.8	693 ± 85.4	35.0 ± 4.0	90.0 ± 7.4
15	1	5.1 ± 0.8	11.9 ± 2.0	99.7 ± 16.2	45.6 ± 5.0	11.9 ± 2.0	35.5 ± 2.4	205 ± 18.8	2.7 ± 0.2	18.8 ± 2.3	412 ± 51.1	711 ± 129	28.8 ± 5.1	80.2 ± 5.5
	2	6.1 ± 1.1	14.1 ± 2.2	95.5 ± 15.2	53.2 ± 5.1	14.4 ± 2.0	30.5 ± 3.0	211 ± 20.0	3.2 ± 0.4	20.7 ± 2.7	386 ± 35.5	666 ± 120	32.7 ± 4.5	91.1 ± 4.8
	3	5.9 ± 1.4	15.2 ± 3.4	107 ± 11.2	55.1 ± 7.1	13.3 ± 1.8	29.6 ± 2.8	188 ± 16.4	3.1 ± 0.5	22.1 ± 3.0	377 ± 27.4	685 ± 55.7	40.2 ± 6.2	90.7 ± 9.0
	4	5.7 ± 1.0	12.2 ± 2.2	111 ± 20.7	50.0 ± 4.2	12.2 ± 3.0	31.1 ± 3.7	190 ± 20.3	1.9 ± 0.3	16.6 ± 3.1	407 ± 33.3	714 ± 76.4	34.4 ± 4.0	76.4 ± 5.6
	5	4.8 ± 1.0	14.0 ± 2.2	94.4 ± 10.2	49.9 ± 3.9	10.9 ± 2.1	30.1 ± 1.9	166 ± 21.1	4.0 ± 2.4	18.5 ± 2.0	401 ± 40.2	701 ± 102	36.6 ± 4.1	102 ± 13.4
	6	4.9 ± 0.9	13.9 ± 2.4	95.6 ± 9.9	50.0 ± 5.1	13.4 ± 4.1	28.8 ± 2.5	203 ± 20.1	8.5 ± 1.8*	19.6 ± 2.1	412 ± 36.4	700 ± 85.2	35.8 ± 2.8	111 ± 24.1
	7	5.1 ± 1.4	11.7 ± 1.8	112 ± 14.5	51.2 ± 4.0	11.8 ± 2.7	34.4 ± 3.2	202 ± 16.5	3.5 ± 0.9	20.1 ± 2.2	388 ± 28.5	688 ± 84.5	41.1 ± 3.3	89.7 ± 7.4
	8	5.2 ± 2.0	12.2 ± 2.0	109 ± 12.2	46.6 ± 3.7	14.0 ± 2.1	30.0 ± 2.8	189 ± 27.4	4.6 ± 0.8	19.7 ± 3.0	375 ± 30.0	690 ± 71.1	40.7 ± 2.9	92.2 ± 12.7
19	1	5.5 ± 1.6	11.9 ± 1.8	111 ± 10.2	50.1 ± 4.7	12..2 ± 2.3	36.6 ± 2.1	210 ± 22.1	3.2 ± 0.3	17.9 ± 3.1	370 ± 32.1	665 ± 74.1	29.8 ± 1.8	101 ± 9.9
	2	5.6 ± 1.5	10.7 ± 0.9	101 ± 7.7	52.3 ± 6.0	13.0 ± 2.0	33.2 ± 3.0	196 ± 24.7	3.3 ± 0.2	18.4 ± 2.1	366 ± 40.1	674 ± 101	31.0 ± 2.7	85.6 ± 7.7
	3	6.1 ± 1.4	13.3 ± 1.3	92.2 ± 7.6	60.7 ± 7.1	14.1 ± 2.5	32.7 ± 1.9	185 ± 30.2	4.1 ± 0.6	19.5 ± 2.4	405 ± 62.1	712 ± 54.1	37.4 ± 4.4	76.3 ± 6.1
	4	6.0 ± 1.5	14.1 ± 2.2	90.7 ± 6.6	48.5 ± 5.8	12.9 ± 1.9	37.4 ± 3.5	178 ± 25.1	4.2 ± 1.1	20.7 ± 1.9	400 ± 36.1	720 ± 64.2	35.5 ± 3.5	80.1 ± 7.1
	5	4.7 ± 1.0	10.9 ± 1.8	88.7 ± 9.2	55.6 ± 6.1	11.7 ± 2.0	29.9 ± 4.1	213 ± 26.4	3.6 ± 0.3	20.1 ± 2.2	408 ± 29.6	704 ± 52.3	29.9 ± 3.1	89.9 ± 6.5
	6	5.0 ± 0.9	11.4 ± 2.0	80.1 ± 10.2	54.4 ± 6.1	12.2 ± 1.5	35.5 ± 3.0	222 ± 31.4	9.7 ± 1.3*	28.3 ± 2.1*	419 ± 40.5	685 ± 58.1	33.0 ± 3.2	90.2 ± 6.4
	7	5.3 ± 0.8	12.2 ± 1.8	116 ± 12.3	50.7 ± 7.1	13.3 ± 2.9	34.7 ± 3.0	187 ± 20.0	3.1 ± 0.4	19.5 ± 2.7	395 ± 40.1	700 ± 88.4	34.7 ± 2.6	127 ± 9.1*
	8	5.5 ± 1.4	13.3 ± 2.7	110 ± 13.0	48.7 ± 4.4	15.5 ± 3.0	36.6 ± 2.8	196 ± 18.5	5.0 ± 0.8*	23.5 ± 3.0	378 ± 45.2	699 ± 85.8	38.8 ± 5.0	135 ± 16.7*

Serum cytokine levels for each treatment group at each time point of the gold allergy study. $n = 4$ per group, $p < 0.05$.
*Indicates statistically significant over group 5 control.

Table 6. Gold allergy model BALF cytokine levels (pg/mL).

Time point (days)	Tx group	Th1/Th17 cytokines							Th2 cytokines				Other	
		IFN-γ	IL-2	IL-12p40	IL-12p70	IL-17	TNF-α	GM-CSF	IL-4	IL-5	IL-13	Eotaxin	IL-6	IL-10
11	1	3.3 ± 0.3	6.0 ± 0.4	112 ± 15.4	36.4 ± 3.0	1.2 ± 0.1	4.0 ± 0.3	3.3 ± 0.3	5.5 ± 0.4	5.2 ± 0.4	2.6 ± 0.6	3.4 ± 0.5	2.5 ± 0.2	2.0 ± 0.2
	2	2.9 ± 0.4	5.5 ± 0.3	101 ± 9.6	29.8 ± 1.8	0.9 ± 0.1	3.6 ± 0.3	2.8 ± 0.2	6.2 ± 0.7	6.1 ± 0.8	3.0 ± 1.0	3.5 ± 0.3	3.1 ± 0.3	2.1 ± 0.3
	3	2.2 ± 0.2	5.4 ± 0.3	98.5 ± 7.7	31.1 ± 3.0	1.0 ± 0.2	3.8 ± 0.4	2.4 ± 0.1	6.0 ± 1.1	5.8 ± 0.5	2.5 ± 0.4	3.0 ± 0.2	3.0 ± 0.2	2.2 ± 0.2
	4	2.4 ± 0.2	6.1 ± 1.0	95.4 ± 8.0	32.2 ± 2.8	1.3 ± 0.2	4.2 ± 0.5	3.0 ± 0.3	5.9 ± 0.7	5.5 ± 0.8	3.2 ± 0.3	3.1 ± 0.3	2.8 ± 0.2	2.2 ± 0.3
	5	3.0 ± 0.2	5.2 ± 0.6	88.7 ± 9.5	35.5 ± 3.3	2.0 ± 0.2	4.5 ± 0.2	4.2 ± 0.9	4.8 ± 0.4	7.1 ± 0.5	3.0 ± 0.2	2.8 ± 0.3	2.6 ± 0.4	1.8 ± 0.2
	6	3.2 ± 0.4	5.5 ± 0.5	80.1 ± 7.7	27.7 ± 2.9	1.3 ± 0.2	4.0 ± 0.3	3.6 ± 0.5	4.9 ± 0.5	6.5 ± 0.5	3.1 ± 0.2	4.1 ± 0.4	3.3 ± 0.3	3.2 ± 0.3
	7	2.4 ± 0.2	6.1 ± 0.6	114 ± 12.3	34.0 ± 2.5	1.1 ± 0.1	3.9 ± 0.3	2.9 ± 0.8	5.2 ± 0.5	5.9 ± 0.5	1.9 ± 0.2	4.0 ± 0.5	3.0 ± 0.3	3.0 ± 0.3
	8	2.7 ± 0.1	5.8 ± 0.4	122 ± 10.4	33.3 ± 2.8	2.1 ± 0.3	2.8 ± 0.3	3.1 ± 0.6	5.5 ± 0.4	6.0 ± 0.5	2.2 ± 0.2	3.3 ± 0.3	3.1 ± 0.5	1.9 ± 0.4
15	1	2.8 ± 0.2	4.8 ± 0.5	120 ± 12.2	30.1 ± 2.5	0.8 ± 0.1	4.0 ± 0.4	3.3 ± 0.5	6.1 ± 0.5	5.7 ± 0.3	2.8 ± 0.3	4.2 ± 0.6	3.3 ± 0.5	2.6 ± 0.5
	2	3.0 ± 0.3	6.2 ± 0.8	122 ± 15.4	30.0 ± 3.5	0.9 ± 0.2	3.5 ± 0.3	3.6 ± 0.4	6.6 ± 0.7	4.9 ± 0.6	2.9 ± 0.2	5.0 ± 0.8	2.9 ± 0.2	2.2 ± 0.1
	3	3.1 ± 0.3	6.0 ± 0.8	104 ± 10.7	28.8 ± 3.5	0.8 ± 0.2	3.2 ± 0.3	4.4 ± 0.8	5.3 ± 0.5	7.2 ± 0.5	1.8 ± 0.3	2.8 ± 0.3	3.0 ± 0.5	2.5 ± 0.3
	4	2.5 ± 0.2	5.5 ± 1.0	98.7 ± 12.2	29.9 ± 2.8	1.4 ± 0.3	3.1 ± 0.3	2.9 ± 0.3	4.8 ± 0.4	6.6 ± 0.4	3.3 ± 0.3	3.3 ± 0.3	3.5 ± 0.8	3.1 ± 0.3
	5	2.6 ± 0.2	5.4 ± 0.5	92.5 ± 8.5	35.5 ± 4.0	1.5 ± 0.2	4.2 ± 0.3	2.6 ± 0.3	5.7 ± 0.5	5.9 ± 0.4	1.9 ± 0.2	4.0 ± 0.4	2.8 ± 0.4	2.6 ± 0.2
	6	2.7 ± 0.3	4.9 ± 0.5	90.1 ± 8.5	28.6 ± 2.9	0.9 ± 0.1	4.4 ± 0.4	3.0 ± 0.2	5.5 ± 0.5	5.5 ± 0.5	2.5 ± 0.3	4.2 ± 0.4	16.2 ± 2.5*	2.7 ± 0.3
	7	2.4 ± 0.3	6.1 ± 0.8	96.6 ± 10.0	31.1 ± 3.5	0.8 ± 0.1	4.5 ± 0.5	10.1 ± 0.8*	6.3 ± 0.6	5.0 ± 0.4	2.7 ± 0.2	3.9 ± 0.4	4.0 ± 0.6	2.9 ± 0.3
	8	2.5 ± 0.2	5.5 ± 0.5	116 ± 13.3	32.2 ± 2.7	1.0 ± 0.3	3.7 ± 0.3	3.2 ± 0.5	6.0 ± 0.3	6.8 ± 0.5	2.2 ± 0.1	5.0 ± 0.4	3.9 ± 0.3	2.4 ± 0.2
19	1	3.0 ± 0.3	5.2 ± 0.4	96.7 ± 8.6	32.2 ± 3.5	1.0 ± 0.1	5.0 ± 0.5	2.8 ± 0.4	6.1 ± 0.5	5.9 ± 0.6	2.9 ± 0.3	5.1 ± 0.6	4.1 ± 0.6	2.5 ± 0.2
	2	3.1 ± 0.4	4.8 ± 0.6	100 ± 8.6	29.6 ± 2.0	1.1 ± 0.2	4.0 ± 0.4	2.6 ± 0.5	5.7 ± 0.5	4.8 ± 0.4	3.3 ± 0.2	4.4 ± 0.5	3.2 ± 1.0	2.6 ± 0.2
	3	2.8 ± 0.3	5.8 ± 0.6	119 ± 9.6	36.7 ± 4.0	1.3 ± 0.2	3.9 ± 0.4	3.5 ± 0.3	4.7 ± 0.5	6.2 ± 0.5	3.0 ± 0.3	4.4 ± 0.6	2.8 ± 0.2	3.3 ± 0.4
	4	2.9 ± 0.2	6.3 ± 0.9	111 ± 7.4	32.2 ± 2.9	1.2 ± 0.1	4.4 ± 0.5	4.1 ± 0.6	4.9 ± 0.5	7.0 ± 0.6	4.1 ± 0.3	3.8 ± 0.7	2.9 ± 0.3	3.1 ± 0.5
	5	3.5 ± 0.6	6.8 ± 1.2	88.5 ± 6.4	31.1 ± 4.2	1.8 ± 0.2	4.6 ± 0.4	3.6 ± 0.8	6.6 ± 0.7	5.8 ± 0.3	2.6 ± 0.2	2.9 ± 0.3	3.2 ± 0.3	2.0 ± 0.1
	6	17.0 ± 3.2@	5.7 ± 0.5	113 ± 15.4	28.8 ± 3.0	2.2 ± 0.1	5.2 ± 0.5	3.5 ± 0.7	5.5 ± 0.6	5.5 ± 0.3	2.5 ± 0.2	3.6 ± 0.4	6.2 ± 1.0	2.2 ± 0.2
	7	6.2 ± 1.5*	15.5 ± 2.5*	107 ± 10.6	62.1 ± 4.5*	0.8 ± 0.2	5.0 ± 0.3	5.4 ± 0.8	5.4 ± 0.5	6.6 ± 0.3	3.6 ± 0.3	4.1 ± 0.4	4.2 ± 0.8	3.0 ± 0.3
	8	14.7 ± 2.0@	11.9 ± 1.6*	95.5 ± 8.7	55.6 ± 4.9*	1.4 ± 0.2	3.8 ± 0.4	4.0 ± 0.8	6.3 ± 0.6	6.9 ± 0.6	3.3 ± 0.3	5.2 ± 0.5	4.4 ± 0.6	2.8 ± 0.2

Bronchoalveolar lavage fluid (BALF) cytokine levels for each treatment group at each time point of the gold allergy study. $n = 4$ per group, $p < 0.05$.
*Indicates statistically significant over group 5 control, @indicates statistical significance over groups 5 and 7.

physicochemical properties other than size also influence the immunological activity of metals (Roach, Stefaniak, and Roberts 2019). Discrepancies in the magnitude of lymphocyte activation appeared specifically associated with variations in dissolution behavior between the LLNA test materials (Fowler 1987). As the major antigenic determinant responsible for metal-induced ACD, the greater propensity for release of haptenic ions by soluble metal compounds underlies the increased risk for sensitization associated with these formulations (Garner 2004). Accordingly, the highest SI was associated with $AuCl_3$ – one of several soluble gold salts known to release large quantities of haptenic ions upon skin exposure and subsequent proliferation of lymphocytes in the draining lymph nodes (Basketter et al. 1999; Ikarashi, Kaniwa, and Tsuchiya 2002; Kaur et al. 2006; Moller et al. 2005). By comparison, Au and AuNP did not induce significant expansion of the lymph nodes, consistent with the lack of immunogenicity associated with metallic and insoluble forms of gold (Liden, Nordenadler, and Skare 1998). These materials are particularly resistant to dissolution, and thus, generally constitute ineffective sources of ACD-inducing doses of haptenic ions (Wang and Dai 2013).

In the dose-response study, no signs of overt lung toxicity were observed following AuNP aspiration at any time point, irrespective of dose (Table 2). This finding is consistent with other studies that have demonstrated general biocompatibility of AuNP in the respiratory tract (Gosens et al. 2010; Han et al. 2015; Schulz et al. 2012). The only parameter altered in response to exposure was MLN size in animals administered the highest AuNP dose (Figure 5). This increase in MLN cellularity was associated with an elevated percentage of both CD4+ T-cells and B-cells, which became evident at day 4 and persisted until day 8. The immunological implications of this finding cannot be discerned from the scope of this study; however, since CD4+ T-cells and B-cells are both lymphocyte subpopulations traditionally associated with critical effector functions in type 2 immune responses, the expansion of these populations may have implications for ensuing antigen encounters (Kubo 2017). As illustrated by several other studies, pulmonary AuNP exposure can induce alterations in the local microenvironment which, upon subsequent antigen uptake, prime the immune system to generate polarized antigen-specific responses (Dykman et al. 2018; Seydoux et al. 2016).

Overall, the results from the LLNA and AuNP dose-response studies indicate that AuNP are not likely to induce allergic sensitization via the skin or respiratory tract. A similar lack of immune responsivity was also apparent in non-sensitized animals of the allergy study; however, aspiration of gold particles caused alterations in several notable immune endpoints in previously-sensitized animals, suggesting that established, gold-specific immunological memory is a critical mediator of lung responses to Au/AuNP.

Unlike most other metal allergens known to cause ACD (e.g. nickel, cobalt, chromium), gold has not been previously implicated in any cases of metal-induced asthma. In fact, it remains largely unknown if respiratory exposure to gold is associated with any local or systemic immune effects. Interestingly, nearly all adverse pulmonary immune responses caused by gold have been reported in human subjects receiving systemic gold salts for the treatment of rheumatoid arthritis (Eisler 2003). One such response – referred to as 'gold lung' – is a condition often described as a variant of hypersensitivity pneumonitis, wherein inflammation of the alveolar mucosa is orchestrated by gold-reactive T-lymphocytes (Bogaert et al. 2009; Sforza and Marinou 2017). Although it remains unclear if inhalation exposures to the metal can induce similar adaptive immune responses as those responsible for gold lung, several findings from the gold allergy study suggest that similar mechanisms may be involved.

First, the gold allergy study and existing gold lung case report both assert a critical association between established skin sensitivity to gold and lung responsivity to the metal. The vast majority of patients that develop gold lung exhibit prior patch test positivity and report a history of dermal eruptions following systemic administration of gold salts (Garcia et al. 1987; Paako et al. 1984). In many cases, systemic sensitization occurs during gold therapy, following which, the newly-generated populations of gold-specific T-cells mediate ACD-like reactions upon subsequent exposures to gold. In some cases, gold deposits that accumulate in lung tissue during treatment can trigger the recruitment

of these cells to the airways, initiating the development of gold lung (Tomioka and King 1997). In accordance with this mechanism, concurrent presentations of ACD and gold lung frequently occur in patients because the same gold-specific effector T-cell populations generated during sensitization are responsible for orchestrating the pathogenesis of both conditions. In the gold allergy model, the dependence of Au/AuNP immunological activity on prior sensitization implies a similar role for gold-specific adaptive immunity in the observed responses.

The BAL lymphocyte responses characterized in the gold allergy study also bear many similarities to findings reported in human cases of the gold lung. Consistent with the cell-mediated mechanisms underlying presentations of the gold lung, lymphocyte predominance within the BAL (>25%) is often cited as a diagnostic marker used for clinical evaluation of suspected cases (Tomioka and King 1997). Although the magnitude of lymphocyte influx in sensitized animals of the gold allergy study was not nearly as pronounced as responses characteristically seen in gold lung cases, gold exposure did induce significant elevations in BAL lymphocytes in a surface area-dependent manner.

Furthermore, the phenotypic profile of BAL lymphocytes represents another immunological parameter similarly modulated in the context of the gold lung and the allergy model. Gold-induced ACD is known to involve effector functions mediated by gold-reactive T-cells bearing both CD4+ and CD8+ phenotypes (Chen and Lampel 2015; Hashizume et al. 2008). Both T-cell subsets are also increasingly recruited to the airways in gold lung patients (Agarwal, Sharma, and Malaviya 1989; Breton et al. 1993; Matsumura, Miyake, and Ishida 1992; McCormick et al. 1980). However, extensive evidence suggests that, similar to the immunological mechanisms involved in hypersensitivity pneumonitis, the pathogenesis of gold lung exhibits a greater dependence on the activities of CD8+ T-cells than that of CD4+ T-cells. Accordingly, an inverted BAL CD4:8 T-cell ratio (<1) is often used as a biomarker to confirm suspected cases of the gold lung in humans (Evans et al. 1987). Interestingly, a similar decreased CD4:8 BAL T-cell ratio was observed in the gold allergy study, but only in group 7 animals, which were exposed to the high dose of AuNP. Animals of groups 6 and 8 exhibited elevated numbers of total BAL lymphocytes, but the increase involved a preferential influx of CD4+ T-cells. This finding suggests that gold may induce lung immune responses mediated by phenotypically-distinct subsets of T-cells in sensitized individuals, wherein preferential recruitment of CD4/CD8+ T-cells is dependent on the dose metric of surface area.

Although patients afflicted with gold lung are known to exhibit BAL and peripheral lymphocyte reactivity to gold, T-cell reactivity was not directly assessed in the allergy study (Tomioka and King 1997). Despite this, the sensitization state-dependent recruitment of lymphocytes to the airways after respiratory gold exposure suggests the specificity of these cells for the metal. Additionally, concentrations of several cytokines (e.g. IFN-γ, IL-2) known to be released by gold-specific T-cells following activation were upregulated in the BALF of sensitized animals (Christiansen et al. 2006; Minang et al. 2006).

Collectively, these findings suggest that the lack of immunogenicity associated with Au and AuNP during the sensitization phase of metal allergy does not necessarily implicate a similar absence of activity in the context of allergic elicitation. Moreover, the influence of specific nanomaterial physicochemical properties may differ with respect to allergic processes in the skin and lungs. Dissolution behavior appeared to be a property responsible for limiting skin sensitizing potential, but the elicitation of adaptive immune responses in the airways was best correlated with the dose parameter of surface area. Although this observation might reflect an association between nanomaterial surface area and dissolution rate, irrespectively, the propensity for ion release presented a barrier of less impact during the elicitation phase. This finding is consistent with the knowledge that the threshold of exposure required to elicit T-cell-mediated metal-specific allergic responses can be 100 to 1000-fold lower than that required to induce sensitization (Larsen et al. 1980).

Metal-induced ACD is most commonly associated with prototypical Th1-polarized cell-mediated mechanisms of hypersensitivity – a state of immune reactivity known to involve distinctive cell types, signaling pathways, and effector molecules that negatively regulate Th2/type 2 immune activity

(Licona-Limón et al. 2013; Romagnani 2004). In accordance with this knowledge, the observation that all gold-sensitized groups exhibited higher levels of serum IgE than non-sensitized groups at day 11 was an unexpected finding in the allergy study; however, a similar increase in circulating IgE has been reported in other studies after dermal sensitization with gold sodium thiosulfate (Ikarashi, Kaniwa, and Tsuchiya 2002). In a similar context, gold-reactive T-cells isolated from sensitized individuals have been shown to produce seemingly contradictory cytokine profiles (mixed Th1/Th2, Th0/Tc1) following stimulation *ex vivo* (Hashizume et al. 2008; Minang et al. 2006). These observations highlight the often oversimplified classification schemes applied to allergic responses and emphasize the potential influence of previously-overlooked mediators (e.g. regulatory subsets of innate and immune cells, innate lymphoid cells) in metal allergy (McKenzie 2014).

Similar complexities also likely underlie the observation that subsequent aspirations of gold only caused further elevations in serum IgE in groups 6 and 8 – sensitized animals exposed to the lower surface area-based dose of Au/AuNP. Moreover, the lower surface area-based doses of Au/AuNP implicated in this effect were not associated with similar increases in IgE production by non-sensitized animals. Likewise, the gold aspiration-induced increases in IgE level appear not only dependent on the gold aspiration dose surface area, but also on sensitization status. Gold has rarely been associated with immediate-type hypersensitivity responses or the development of specific IgE, and since the specificity of IgE was not determined in this study, the direct implications of this observation remain unclear; however, future efforts should consider the potential involvement of mixed type allergic responses with respect to metal allergy and metal nanomaterial exposures.

Conclusion

Overall, the results from these studies suggest that 30 nm AuNP do not constitute a significant risk for dermal sensitization or pulmonary immune responses following acute exposure; however, a notable increase in immune responsivity to the particles was observed in a state of established contact sensitivity to gold. Subsequent immune effects appeared best correlated to the surface area of the administered dose, wherein the higher dose of AuNP was associated with many response features resembling those seen in the gold lung, a T-cell-mediated hypersensitivity condition known to occur in some patients receiving systemic gold therapy. These results imply that individuals with existing contact allergy may be at increased risk for adverse immune effects following respiratory exposure to AuNP or other gold materials. Ultimately, as efforts to characterize the immunotoxic potential of nanomaterials continue, the prevalence of metal hypersensitivity within the general population should be considered as a potential predisposing risk factor for adverse effects of metal nanomaterial exposure.

Disclosure statement

No potential conflict of interest was reported by the author(s).

Funding

This work was supported by National Institute for Occupational Safety and Health and the American Foundation for Pharmaceutical Education.

References

Aaron, S., P. Davis, and J. Percy. 1985. "Neutropenia Occurring during the Course of Chrysotherapy: A Review of 25 Cases." *The Journal of Rheumatology* 12 (5): 897–899.

Agarwal, R., S. K. Sharma, and A. N. Malaviya. 1989. "Gold-Induced Hypersensitivity Pneumonitis in a Patient with Rheumatoid Arthritis." *Clinical and Experimental Rheumatology* 7 (1): 89–90.

American Society for Testing and Materials International. 2002. *Standard Test Method for Metal Powder Specific Surface Area by Physical Adsorption*. West Conshohocken, PA: ASTM International.

Bancos, S., D. L. Stevens, and K. M. Tyner. 2015. "Effect of Silica and Gold Nanoparticles on Macrophage Proliferation, Activation Markers, Cytokine Production, and Phagocytosis in Vitro." *International Journal of Nanomedicine* 10: 183–206. doi:10.2147/IJN.S72580.

Barreto, E., M. F. Serra, R. V. Dos Santos, C. E. Dos Santos, J. Hickmann, A. C. Cotias, C. R. Pao, S. G. Trindade, V. Schimidt, C. Giacomelli et al. 2015. "Local Administration of Gold Nanoparticles Prevents Pivotal Pathological Changes in Murine Models of Atopic Asthma." *Journal of*

Biomedical Nanotechnology 11 (6): 1038–1050. doi:10.1166/jbn.2015.2024.

Basketter, D., P. Evans, R. Fielder, G. Gerberick, R. Dearman, and I. Kimber. 2002. "Local Lymph Node Assay—Validation, Conduct and Use in Practice." Food *and Chemical Toxicology* 40 (5): 593–598. doi:10.1016/S0278-6915(01)00130-2.

Basketter, D. A., L. J. Lea, K. J. Cooper, C. A. Ryan, G. F. Gerberick, R. J. Dearman, and I. Kimber. 1999. "Identification of Metal Allergens in the Local Lymph Node Assay." *American Journal of Contact Dermatitis: Official Journal of the American Contact Dermatitis Society* 10 (4): 207–212. doi:10.1053/AJCD01000207.

Bogaert, P., K. G. Tournoy, T. Naessens, and J. Grooten. 2009. "Where Asthma and Hypersensitivity Pneumonitis Meet and Differ: Noneosinophilic Severe Asthma." *The American Journal of Pathology* 174 (1): 3–13. doi:10.2353/ajpath.2009.071151.

Breton, J., V. Westeel, G. Garnier, and J. Louis. 1993. "Gold Salt-Induced Pneumonia and CD4 Alveolitis." *J Revue de Pneumologie Clinique* 49 (1): 27–29.

Chen, J. K., and H. P. Lampel. 2015. "Gold Contact Allergy: Clues and Controversies." *Dermatitis: Contact, Atopic, Occupational, Drug* 26 (2): 69–77. doi:10.1097/DER.0000000000000101.

Chia-Hui, L., S. Shih-Han, C. Yu-Shiun, M. H. Saber, O. Andrei Aleksandrovich, C. Wen Liang, and G. S. Huang. 2014. "Gold Nanoparticles Regulate the blimp1/pax5 Pathway and Enhance Antibody Secretion in B-Cells." *Nanotechnology* 25 (12): 125103.

Christiansen, J., G. Farm, R. Eid-Forest, C. Anderson, K. Cederbrant, and P. Hultman. 2006. "Interferon-Gamma Secreted from Peripheral Blood Mononuclear Cells as a Possible Diagnostic Marker for Allergic Contact Dermatitis to Gold." *Contact Dermatitis* 55 (2): 101–112. doi:10.1111/j.1600-0536.2006.00908.x.

Davis, M. D. P., M. Z. Wang, J. A. Yiannias, J. H. Keeling, S. M. Connolly, D. M. Richardson, and S. A. Farmer. 2011. "Patch Testing with a Large Series of Metal Allergens: Findings from More than 1,000 Patients in One Decade at Mayo Clinic." *Dermatitis* 22 (5): 256–271.

Dearman, R., D. Basketter, and I. Kimber. 1999. "Local Lymph Node Assay: Use in Hazard and Risk Assessment." *Journal of Applied Toxicology* 19 (5): 299–306. doi:10.1002/(SICI)1099-1263(199909/10)19:5<299::AID-JAT591>3.0.CO;2-C.

Dreaden, E. C., L. A. Austin, M. A. Mackey, and M. A. El-Sayed. 2012. "Size Matters: Gold Nanoparticles in Targeted Cancer Drug Delivery." *Therapeutic Delivery* 3 (4): 457–478. doi:10.4155/tde.12.21.

Dykman, L. A., S. A. Staroverov, A. S. Fomin, V. A. Khanadeev, B. N. Khlebtsov, and V. A. Bogatyrev. 2018. "Gold Nanoparticles as an Adjuvant: Influence of Size, Shape, and Technique of Combination with CpG on Antibody Production." *International Immunopharmacology* 54: 163–168. doi:10.1016/j.intimp.2017.11.008.

Eisler, R. 2003. "Chrysotherapy: A Synoptic Review." *Inflammation Research* 52 (12): 487–501. doi:10.1007/s00011-003-1208-2.

Evans, D. E., L. A. Turkevich, C. T. Roettgers, G. J. Deye, and P. A. Baron. 2013. "Dustiness of Fine and Nanoscale Powders." *The Annals of Occupational Hygiene* 57 (2): 261–277. doi:10.1093/annhyg/mes060.

Evans, R. B., D. B. Ettensohn, F. Fawaz-Estrup, E. V. Lally, and S. R. Kaplan. 1987. "Gold Lung: Recent Developments in Pathogenesis, Diagnosis, and Therapy." *Seminars in Arthritis and Rheumatism* 16 (3): 196–205. doi:10.1016/0049-0172(87)90022-9.

Fowler, J., Jr., J. Taylor, F. Storrs, E. Sherertz, R. Rietschel, M. Pratt, C. G. Mathias, J. Marks, H. Maibach, A. Fransway, et al. 2001. "Gold Allergy in North America." *American Journal of Contact Dermatitis* 12 (1): 3–5.

Fowler, J. F. 1987. "Selection of Patch Test Materials for Gold Allergy." *Contact Dermatitis* 17 (1): 23–25. doi:10.1111/j.1600-0536.1987.tb02639.x.

Garcia, J. G., A. Munim, K. M. Nugent, M. Bishop, P. Hoie-Garcia, N. Parhami, and B. A. Keogh. 1987. "Alveolar Macrophage Gold Retention in Rheumatoid Arthritis." *The Journal of Rheumatology* 14 (3): 435–438.

Garner, L. A. 2004. "Contact Dermatitis to Metals." *Dermatologic Therapy* 17 (4): 321–327. doi:10.1111/j.1396-0296.2004.04034.x.

Gosens, I., J. A. Post, L. J. de la Fonteyne, E. H. Jansen, J. W. Geus, F. R. Cassee, and W. H. de Jong. 2010. "Impact of Agglomeration State of nano- and submicron sized gold particles on pulmonary inflammation." *Particle and Fibre Toxicology* 7 (1): 37. doi:10.1186/1743-8977-7-37.

Guo, J., K. Rahme, Y. He, L.-L. Li, J. D. Holmes, and C. M. O'Driscoll. 2017. "Gold Nanoparticles Enlighten the Future of Cancer theranostics." *International Journal of Nanomedicine* 12: 6131–6152. doi:10.2147/IJN.S140772.

Han, S. G., J. S. Lee, K. Ahn, Y. S. Kim, J. K. Kim, J. H. Lee, J. H. Shin, K. S. Jeon, W. S. Cho, N. W. Song, et al. 2015. "Size-Dependent Clearance of Gold Nanoparticles from Lungs of Sprague-Dawley Rats after Short-Term Inhalation Exposure." *Archives of Toxicology* 89 (7): 1083–1094. doi:10.1007/s00204-014-1292-9.

Hashizume, H., N. Seo, T. Ito, M. Takigawa, and H. Yagi. 2008. "Promiscuous Interaction between Gold-Specific T Cells and APCs in Gold Allergy." *Journal of Immunology* 181 (11): 8096–8102. doi:10.4049/jimmunol.181.11.8096.

Highton, J., G. S. Panayi, P. Shepherd, J. Griffin, and T. Gibson. 1981. "Changes in Immune Function in Patients with Rheumatoid Arthritis following Treatment with Sodium Aurothiomalate." *Annals of the Rheumatic Diseases* 40 (3): 254–262. doi:10.1136/ard.40.3.254.

Hunter, T. 1985. "Hypogammaglobulinaemia Associated with Gold Therapy." *Annals of the Rheumatic Diseases* 44 (3): 212. doi:10.1136/ard.44.3.212-a.

Hussain, S., J. A. J. Vanoirbeek, K. Luyts, V. De Vooght, E. Verbeken, L. C. J. Thomassen, J. A. Martens, D. Dinsdale, S. Boland, F. Marano, et al. 2011. "Lung Exposure to Nanoparticles Modulates an Asthmatic Response in a

Mouse model." *European Respiratory Journal* 37 (2): 299–309. doi:10.1183/09031936.00168509.

Ikarashi, Y., M. Kaniwa, and T. Tsuchiya. 2002. "Sensitization Potential of Gold Sodium Thiosulfate in Mice and guinea Pigs." *Biomaterials* 23 (24): 4907–4914. doi:10.1016/s0142-9612(02)00250-8.

Karlberg, A. T., M. A. Bergstrom, A. Borje, K. Luthman, and J. L. Nilsson. 2008. "Allergic Contact dermatitis-formation, structural requirements, and reactivity of skin sensitizers." *Chemical Research in Toxicology* 21 (1): 53–69. doi:10.1021/tx7002239.

Kaur, S., M. Eisen, K. Leiger, and K. Injarabian. 2006. "Screening for Gold Allergy among Dental Clinic Employees and Patch Test Population." *Contact Dermatitis* 54 (3): 172–173. doi:10.1111/j.0105-1873.2006.0739e.x.

Kim, J. S., K. S. Song, J. H. Sung, H. R. Ryu, B. G. Choi, H. S. Cho, J. K. Lee, and I. J. Yu. 2013. "Genotoxicity, Acute Oral and Dermal Toxicity, Eye and Dermal Irritation and Corrosion and Skin Sensitisation Evaluation of Silver Nanoparticles." *Nanotoxicology* 7 (5): 953–960. doi:10.3109/17435390.2012.676099.

Kubo, M. 2017. "Innate and Adaptive Type 2 Immunity in Lung Allergic Inflammation." *Immunological Reviews* 278 (1): 162–172. doi:10.1111/imr.12557.

Kumar, P., and I. Roy. 2016. "Applications of Gold Nanoparticles in Clinical Medicine." *International Journal of Pharmacy and Pharmaceutical Sciences* 8 (7): 9–16.

Larsen, F. S., and F. Brandrup. 1980. "Nickel Release from Metallic Buttons in Blue Jeans." *Contact Dermatitis* 6 (4): 298–299.

Licona-Limón, P., L. K. Kim, N. W. Palm, and R. A. Flavell. 2013. "TH2, Allergy and Group 2 Innate Lymphoid Cells." *Nature Immunology* 14 (6): 536–542. doi:10.1038/ni.2617.

Liden, C., M. Nordenadler, and L. Skare. 1998. "Metal Release from Gold-Containing Jewelry Materials: No Gold Release Detected." *Contact Dermatitis* 39 (6): 281–285. doi:10.1111/j.1600-0536.1998.tb05942.x.

Matsumura, Y., A. Miyake, and T. Ishida. 1992. "A case of gold lung with positive lymphocyte stimulation test to gold, using bronchoalveolar lymphocytes." *Nihon Kyobu Shikkan Gakkai Zasshi* 30 (3): 472–477.

McCormick, J., S. Cole, B. Lahirir, F. Knauft, S. Cohen, and T. Yoshida. 1980. "Pneumonitis Caused by Gold Salt Therapy: Evidence for the Role of Cell-Mediated Immunity in Its Pathogenesis." *The American Review of Respiratory Disease* 122 (1): 145–152. doi:10.1164/arrd.1980.122.1.145.

McKenzie, A. N. 2014. "Type-2 Innate Lymphoid Cells in Asthma and Allergy." *Annals of the American Thoracic Society* 11 (5): S263–S270. doi:10.1513/AnnalsATS.201403-097AW.

Minang, J. T., I. Arestrom, M. Troye-Blomberg, L. Lundeberg, and N. Ahlborg. 2006. "Nickel, Cobalt, Chromium, Palladium and Gold Induce a Mixed Th1- and Th2-Type Cytokine Response in Vitro in Subjects with Contact Allergy to the Respective Metals." *Clinical and Experimental Immunology* 146 (3): 417–426. doi:10.1111/j.1365-2249.2006.03226.x.

Misharin, A. V., L. Morales-Nebreda, G. M. Mutlu, G. R. S. Budinger, and H. Perlman. 2013. "Flow Cytometric Analysis of Macrophages and Dendritic Cell Subsets in the Mouse Lung." *American Journal of Respiratory Cell and Molecular Biology* 49 (4): 503–510. doi:10.1165/rcmb.2013-0086MA.

Moller, H., I. Ahnlide, B. Gruvberger, and M. Bruze. 2005. "Gold Trichloride and Gold Sodium Thiosulfate as Markers of Contact Allergy to Gold." *Contact Dermatitis* 53 (2): 80–83. doi:10.1111/j.0105-1873.2005.00648.x.

National Institute of Standards Technology (NIST). 2015. *Report of Investigation: Reference Material 8012- Gold Nanoparticles, Nominal 30 nm Diameter*.

Paako, P., S. Anttila, S. Sutinen, and M. Hakala. 1984. "Lysosomal Gold Accumulations in Pulmonary Macrophages." *Ultrastructural Pathology* 7 (4): 289–294. doi:10.3109/01913128409141489.

Piasecka-Zelga, J., P. Zelga, M. Górnicz, P. Strzelczyk, and J. Sójka-Ledakowicz. 2015. "Acute Dermal Toxicity and Sensitization Studies of Novel Nano-Enhanced UV Absorbers." *Journal of Occupational Health* 57 (3): 275–284. doi:10.1539/joh.14-0207-OA.

Roach, K. A., A. B. Stefaniak, and J. R. Roberts. 2019. "Metal Nanomaterials: Immune Effects and Implications of Physicochemical Properties on Sensitization, Elicitation, and Exacerbation of Allergic Disease." *Journal of Immunotoxicology* 16 (1): 87–124. doi:10.1080/1547691X.2019.1605553.

Romagnani, S. 2004. "Immunologic Influences on Allergy and the TH1/TH2 Balance." *The Journal of Allergy and Clinical Immunology* 113 (3): 395–400. doi:10.1016/j.jaci.2003.11.025.

Schulz, M., L. Ma-Hock, S. Brill, V. Strauss, S. Treumann, S. Gröters, B. van Ravenzwaay, and R. Landsiedel. 2012. "Investigation on the Genotoxicity of Different Sizes of Gold Nanoparticles Administered to the Lungs of Rats." *Mutation Research/Genetic Toxicology and Environmental Mutagenesis* 745 (1–2): 51–57. doi:10.1016/j.mrgentox.2011.11.016.

Seydoux, E., L. Rodriguez-Lorenzo, R. A. M. Blom, P. A. Stumbles, A. Petri-Fink, B. M. Rothen-Rutishauser, F. Blank, and C. von Garnier. 2016. "Pulmonary Delivery of Cationic Gold Nanoparticles Boost Antigen-Specific CD4+ T Cell Proliferation." *Nanomedicine: Nanotechnology, Biology, and Medicine* 12 (7): 1815–1826. doi:10.1016/j.nano.2016.02.020.

Sforza, G. G. R., and A. J. C. Marinou. 2017. "Hypersensitivity Pneumonitis: A Complex Lung Disease." *Clinical and Molecular Allergy* 15 (1): 6.

Thakor, A. S., J. Jokerst, C. Zavaleta, T. F. Massoud, and S. S. Gambhir. 2011. "Gold Nanoparticles: A Revival in Precious Metal Administration to Patients." *Nano Letters* 11 (10): 4029–4036. doi:10.1021/nl202559p.

Tomioka, R., and T. E. King. 1997. "Gold-Induced Pulmonary Disease: Clinical Features, Outcome, and Differentiation from Rheumatoid Lung Disease." *American Journal of Respiratory and Critical Care Medicine* 155 (3): 1011–1020. doi:10.1164/ajrccm.155.3.9116980.

Wang, Y., and S. Dai. 2013. "Structural Basis of Metal Hypersensitivity." *Immunologic Research* 55 (1-3): 83–90. doi:10.1007/s12026-012-8351-1.

Yamada, M., M. Foote, and T. W. Prow. 2015. "Therapeutic Gold, Silver, and Platinum Nanoparticles." *Wiley Interdisciplinary Reviews. Nanomedicine and Nanobiotechnology* 7 (3): 428–445. doi:10.1002/wnan.1322.

Yanez-Sedeno, P., and J. Pingarron. 2005. "Gold Nanoparticle-Based Electrochemical Biosensors." *J Analytical Bioanalytical Chemistry* 382 (4): 884–886.

Yoshioka, Y., E. Kuroda, T. Hirai, Y. Tsutsumi, and K. J. Ishii. 2017. "Allergic Responses Induced by the Immunomodulatory Effects of Nanomaterials upon Skin Exposure." *Frontiers in Immunology* 8: 169. doi:10.3389/fimmu.2017.00169.

Zhang, Q., N. Iwakuma, P. Sharma, B. Moudgil, C. Wu, J. McNeill, H. Jiang, and S. Grobmyer. 2009. "Gold Nanoparticles as a Contrast Agent for in Vivo Tumor Imaging with Photoacoustic Tomography." *Nanotechnology* 20 (39): 395102. doi:10.1088/0957-4484/20/39/395102.

Zhang, Y., T. P. Shareena Dasari, H. Deng, and H. Yu. 2015. "Antimicrobial Activity of Gold Nanoparticles and Ionic Gold." *Journal of Environment Science and Health. Part C Environmental Carcinogenesis & Ecotoxicology Reviews* 33 (3): 286–327. doi:10.1080/10590501.2015.1055161.